JBC Papers in Press. Published on November 7, 2011 as Manuscript M111.285205
The latest version is at http://www.jbc.org/cgi/doi/10.1074/jbc.M111.285205

IKKε, STAT1, and IFIT2 define a novel innate immune effector pathway against West Nile virus infection

Olivia Perwitasari[1,2], Hyelim Cho[3], Michael S. Diamond[3,4,5], and Michael Gale, Jr.[1,2,*]
[1]Department of Immunology, [2]Molecular and Cellular Biology Program, University of Washington School of Medicine, Seattle, WA 98195, [3]Department of Molecular Microbiology, [4]Pathology and Immunology, [5]Medicine, Washington University School of Medicine, St. Louis, MO 63110.

Running title: *IFIT2 restriction of WNV infection through IKKε phosphorylation of STAT1*

[*]Address correspondence to: Dr. Michael Gale, Jr., University of Washington School of Medicine, Department of Immunology, Box 357650, Seattle, WA 98195. Phone: (206) 685-7953. Fax: (206) 643-1013. E-mail: mgale@u.washington.edu

Keywords: Interferon, STAT1, IKKε, West Nile virus

Background: IFN activates JAK-STAT signaling, where STAT1 phosphorylation is crucial for ISG induction and expression of IFIT2 to limit West Nile virus infection.
Results: IKKε mediates STAT1 serine 708 phosphorylation exclusive of tyrosine phosphorylation but dependent on nuclear export and ISG synthesis.
Conclusion: IKKε-mediated STAT1 S708 phosphorylation is crucial for IFIT2 expression to control WNV.
Significance: We define a novel anti-WNV innate immune effector pathway.

SUMMARY

West Nile virus is an emerging virus whose virulence is dependent upon viral evasion of interferon (IFN) and innate immune defenses. The actions of IFN-stimulated genes (ISGs) impart control of virus infection but the specific ISGs and regulatory pathways that restrict WNV are not defined. Here we show that IKKε phosphorylation of STAT1 at serine 708 (S708) drives IFIT2 expression to mediate anti-WNV effector function of IFN. WNV infection was enhanced in cells from IKKε-/- or IFIT2-/- mice. In IKKε-/- cells the loss of IFN-induced IFIT2 expression was linked to lack of STAT1 phosphorylation on S708 but not Y701 nor S727. STAT1 S708 phosphorylation occurs independently of IRF-3 but requires signaling through the IFN-α/β receptor as a late event in the IFN-induced innate immune response that coincides with IKKε-responsive ISGs expression. Biochemical analyses show that STAT1 tyrosine dephosphorylation and CRM1-mediated STAT1 nuclear-cytoplasmic shuttling are required for STAT1 S708 phosphorylation. When compared to wt mice, WNV infected IKKε-/- mice exhibit enhanced kinetics of virus dissemination and increased pathogenesis concomitant with loss of STAT1 S708 phosphorylation and IFIT2 expression. Our results define an IFN-induced IKKε signaling pathway of specific STAT1 phosphorylation and IFIT2 expression that imparts innate antiviral immunity to restrict WNV infection and control viral pathogenesis.

West Nile virus (WNV) is an emerging flavivirus that has recently spread into the Western hemisphere from points of origin within Asia, Africa, or the Middle East (1;2). Infection by WNV is now a leading cause of arboviral encephalitis and imparts 4% overall case fatality frequency in the USA (CDC website, http://www.cdc.gov/ncidod/dvbid/westnile/index.htm). Typically maintained within avian reservoirs, WNV is spread to other vertebrates, including humans as dead-end hosts, through mosquito bite. WNV circulates as 2 major lineages and minor clades, with specific clades of lineage 1 representing the emergent and virulent strain in the North America and elsewhere while lineage 2 strains are typically endemic to Africa and Asia and are not known to cause disease in humans (1;3-6). WNV infection is controlled in part through type-I interferon (IFN) immune defenses

Copyright 2011 by The American Society for Biochemistry and Molecular Biology, Inc.

Downloaded from www.jbc.org at NORTHWESTERN UNIV LIBRARY, on December 9, 2011

(7;8). IFN actions comprise a major component of the innate immune response to virus infection, which serves to restrict virus replication and spread in part through the actions of interferon-stimulated genes (ISGs). WNV suppression of IFN signaling is linked to virus dissemination, neuroinvasion, and virulence of emergent lineage 1 strains (8;9).

WNV acutely induces IFN-β expression from infected cells upon engagement of RNA products including viral RNA by the RIG-I-like receptors (RLRs), RIG-I and MDA5 (10-12). The RLRs signal the downstream activation of interferon regulatory factor (IRF)-3 and NF-κB transcription factors through the actions of the IKK-related kinases (Tank binding kinase 1 (TBK1) and inhibitor of κB kinase epsilon (IKKε). As a result, IRF-3 and NF-κB activation drive the expression of IFN-β, other proinflammatory cytokines, chemokines, and direct IRF-3-target genes that confer antiviral and immune-activating functions (13;14). Secreted IFN-β drives the innate immune response characterized by ISG expression. This process is triggered upon IFN-β binding to the interferon receptor (IFNAR) to induce receptor dimerization, autophosphorylation of receptor-associated kinases Tyk2 and JAK1 leading to tyrosine phosphorylation of signal transducer and activator of transcription (STAT)1 at residue Y701, phosphorylation of STAT2, and assembly of the STAT1/STAT2/IRF9 ISGF3 complex (15-18). ISGF3 function is further augmented or sustained by STAT1 serine phosphorylation at residues S727 and S708 (19-21). ISGF3 translocates to the nucleus and triggers the transcription of hundreds of ISGs (13;15). ISG products serve as immunomodulators and restriction factors against virus infection (22-24).

Among the ISGs IFN-induced protein with tetratricopeptide repeats (IFIT)2, also known as ISG54 has been identified as an ISG restriction factor of WNV (23). IFIT2 belongs to the IFIT gene family whose members function to restrict virus infection through alteration of cellular protein synthesis (reviewed in (25)), and IFIT2 mediates these action by inhibiting eIF3 function in translation initiation (26-28). Our recent study revealed that in the absence of IFN, ectopic IFIT2 expression can impose a blockade that ultimately restricts WNV replication. However, emergent WNV can evade IFIT2 restriction through 2'-O modification of the 5' nontranslated region of the viral RNA mediated by the methyltransferase activity of the viral NS5 protein (23). These observations define IFIT2 as a critical host factor of IFN action and WNV restriction, and underscore the IFIT2/WNV interaction as a critical virus/host interface governing innate antiviral immunity and infection outcome.

IFIT2 is expressed after virus infection directly upon IRF-3 activation as well as upon IFN signaling, owing to the presence of both IRF-3 and ISGF3 binding sites in the *Ifit2* promoter (24;29-31). However, STAT1-/- mice failed to induce IFIT2 expression in the CNS following LCMV and WNV-infection *in vivo* (32). Importantly, IFN-induced expression of murine IFIT2 is dependent upon STAT1 S708 phosphorylation, as recently described by TenOever, *et al.* (21). In this respect, *Ifit2* is among a set of ISGs, including *Adar1*, *Mx1*, and *Oas1b* and others, whose promoters lack purine-rich region upstream of their ISRE which otherwise serves as STAT2 binding sites, wherein STAT1 S708 phosphorylation is thought to increase the affinity for STAT1 binding sites to confer gene expression by ISGF3 in the absence of the STAT2 binding site (21). Notably, STAT1 S708 phosphorylation is induced after IFN treatment of cells. However, the temporal relationship of S708 phosphorylation to other STAT1 phosphorylation sites during IFN-stimulation, innate immune responses, or WNV infection is not known. We therefore conducted the current study to define the cell signaling pathway and STAT1 phosphorylation interactions that drive IFN-induced IFIT2 expression for the restriction of WNV infection. Our results reveal an IKKε-dependent pathway of STAT1 S708 phosphorylation whose activation requires IFN signaling for ISG expression and that plays a key role in the temporal regulation of STAT1 phosphorylation and the expression of IFIT2 crucial to the control of WNV infection and immunity.

EXPERIMENTAL PROCEDURES

Cell culture, interferons, viruses – Parental wildtype (wt) 2fTGH fibrosarcoma cells, U3A (2fTGH-derived mutant cells, deficient in STAT1) and U5A (IFRNAR-deficient, provided by Dr. George Stark, Cleveland Clinic), immortalized human PH5CH8 hepatocytes (provided by Dr.

Downloaded from www.jbc.org at NORTHWESTERN UNIV LIBRARY, on December 9, 2011

Nobuyuki Kato, Okayama University, Japan), and human embryonic kidney HEK293 cells were grown in Dulbecco's modified Eagle medium (DMEM) supplemented with 10% fetal bovine serum (FBS), 2 mM L-glutamine, 1 mM sodium pyruvate, antibiotic-antimycotic solution, and 1x nonessential amino acids (complete DMEM). Primary mouse embryonic fibroblasts (MEFs) were isolated from IKKε-/-, IRF-3-/-, IFNAR-/-, IFIT2-/-, and age-matched wt control mice as previously described (7;33), and grown in DMEM. Human IFNα-2a, human IFN-β, and murine IFNβ (PBL InterferonSource) were used at a concentration of 100 IU/ml, while human IFN-γ and IFN-λ1 (PBL InterferonSource) were used at concentrations of 50 ng/ml and 100 ng/ml, respectively. The Madagascar-AnMg798 strain of WNV (WNV-MAD) was obtained from the World Reference Center of Emerging Viruses and Arboviruses and passaged in Vero cells as previously described (8). The Cantell strain of Sendai virus (SenV) was obtained from the Charles River Laboratory. Where indicated, cells were mock treated, treated with IFN, or infected with either WNV-MAD at an MOI of 1 or SenV at 100 HAU/ml for the indicated times before harvesting for immunoblot assay (8;34). Cycloheximide (CHX; Sigma) and Leptomycin B (LMB; Sigma) was used at a concentration of 50 μg/ml and 100nM respectively. Pervanadate was prepared by mixing equal volumes of 50mM H_2O_2 and 50mM sodium orthovanadate to make 50mM pervanadate before adding into growth media for final concentration of 50μM.

Transfection and promoter-Luciferase analyses – pFLAG-IKKε, pFLAG-STAT1 wt, pFLAG-STAT1 Y701F, and pFLAG-STAT1 S727A expression plasmids were gifts from Dr. Curt Horvath (Northwestern University). pFLAG-STAT1 mutant constructs were generated by site-directed mutagenesis using the QuikChange™ XL Site-Directed Mutagenesis Kit (Stratagene) and the following primers: 5'-CAAGACTGAGTTG ATTGCTGTGTCTGAAGTTC-3' (forward) and 5'-GAACTTCAGACACAGCAATCAACTCAG TCTTG-3' (reverse) for S708A; 5'-CAAGACTG AGTTGATTGATGTGTCTGAAGTTCACCCTT CTAGAC-3' (forward) and 5'-GTCTAGAAGG GTGAACTTCAGACACATCAATCAACTCAGT CTTG-3' (reverse) for S708D; 5'-GATGGCCCT AAAGGAACTGGAGAGATCAAGACTGAGTT G-3' (forward) and 5'-CAACTCAGTCTTGATC TCTCCAGTTCCTTTAGGGCCATC-3' (reverse) for Y701E.

pIFIT2-Luc were gifts from and Kineta, Inc. (Seattle); pISG15-Luc and pIFN-β-Luc were described previously (34). pADAR1-CAT was a gift from Dr. Charles Samuel (UCSD) and pADAR1-Luc was generated by subcloning into pGL3 Luciferase reporter vector. Transfections were carried out for 16 hours using Fugene 6 transfection reagent (Roche) and following the manufacturer's instructions. For luciferase analyses, cells were co-transfected with: 1) either the IFN-β-Luciferase, ISG15-Luciferase, or ADAR1-Luciferase construct, 2) CMV-*Renilla*, and 3) the indicated cDNA expression plasmids. Cell extracts were collected at 24 hours post-infection or treatment and analyzed for dual luciferase activity (Promega).

In vivo mouse infection – C57BL/6 (Bl6) wt and IKKε-/- mice were purchased from Jackson Laboratory (21). Mice were bred in the animal facility at the University of Washington under Specific Pathogen Free (SPF) conditions. Experiments using these animals were completed within the approval and guidelines by the University of Washington Institutional Animal Care and Use Committee. IKKε-/- and age-matched wt control mice were inoculated subcutaneously (s.c.) in the left rear footpad with 10^3 or 10^4 PFU of WNV-MAD as previously described (12). Mice were monitored daily for morbidity and mortality. Clinical symptoms were numerically scored: 1-ruffled fur / lethargic / hunched / no paresis; 2-very mild to mild paresis; 3-frank paresis in at least 1 hind limb or mild paresis in 2 hind limbs; 4-severe paresis, still retains feeling and possibly limbic; 5-true paralysis; 6-moribund; 7-dead (12). For the *in vivo* viral burden analysis, infected mice were bled and perfused with 20 ml of phosphate-buffered saline (PBS) following euthanasia. Spleens were collected and homogenized for immunoblot analysis as previously described (12).

Immunoblot analysis – Protein extracts were prepared by lysing cells in RIPA buffer (50 mM Tris HCl [pH 7.5], 150 mM NaCl, 0.5% sodium deoxycholate, 1% NP-40, 1 mM EDTA, and 0.1% sodium dodecyl sulfate) supplemented with 1 μM okadaic acid, 1 μM phosphatase inhibitor cocktail II (Calbiochem), and 10 μM protease inhibitor

Downloaded from www.jbc.org at NORTHWESTERN UNIV LIBRARY, on December 9, 2011

(Sigma), followed by 4°C centrifugation at 16,000 x g for 10 min to clarify the lysate. Equivalent protein amounts were analyzed by SDS-polyacrylamide gel electrophoresis followed by immunoblotting. Affinity-purified rabbit polyclonal anti-STAT1 S708 antibody was generated by repeat-immunization with the STAT1 S708 phospho-specific peptide (YIKTELI{pS}VSEVHP; aa 701-714) (GenScript). The following primary antibodies were used for immunoblot analyses: α-ADAR1 (Abnova); α-IRF-3 (M. David, UCSD); α-IFIT1, α-murine IFIT2 and α-murine IFIT3 (G. Sen, Cleveland Clinic); α-ISG15 (A. Haas, Louisiana State University); α-WNV (Centers for Disease Control and Prevention); α-p-STAT1 Y701, α-p-STAT1 S727, α-STAT1, α-p-IRF-3 (Cell Signaling); α-murine IRF-3 (Invitrogen); α-IKKε (Imgenex); α-PKR (Santa Cruz); α-SenV (Biodesign International); α-FLAG (M2), and α-Tubulin (Sigma). HrP-conjugated goat anti-rabbit, goat anti-mouse, and donkey anti-goat (Jackson Immunoresearch) were used as secondary antibodies.

Immunoprecipitation – Following FLAG-STAT1 reconstitution of U3A cells and IFN-β treatment, cell extracts were immunoprecipitated using α-FLAG (M2)-conjugated agarose beads (Sigma) for 2 hours at 4°C. Samples were then washed three times with RIPA buffer before elution. The eluate was heated for 5 minutes and analyzed by SDS gel electrophoresis and immunoblot. Subsequently, 20 µl of 50% slurry of protein-G agarose beads (Calbiochem) were added and incubated for 2 hours at 4°C. Beads were washed and eluted as described above. Clean-Blot HrP-conjugated IP detection reagent (Thermo Scientific) was used as a secondary antibody for immunoblot assay.

RESULTS

IKKε and IFIT2 impose restriction of WNV infection– To determine the role of IKKε in IFIT2 expression during WNV infection, we evaluated the IFIT2 abundance and virus replication in primary mouse embryonic fibroblasts (MEF) isolated from wt or IKKε-/- mice. For these studies we utilized the avirulent lineage 2 Madagascar strain of WNV (WNV-MAD). As opposed to virulent lineage 1 strains, WNV-MAD lacks the ability to block IFN signaling and is highly sensitive to the innate immune antiviral actions of IFN (8), thus allowing studies of IFN actions against WNV without confounding influences of viral antagonism of the IFN response. As shown in Fig. 1A, WNV infection induced the expression and accumulation of IFIT2 in a manner dependent on IKKε but IFIT1, IFIT3, and PKR were induced by WNV regardless of IKKε. Following WNV infection of wild type MEFs, IFIT2 was expressed at 48 hours post-infection, while IFIT1 and IFIT3 expression was first observed by 24 hours (Fig. S1). However, virus-induced expression of IFIT2 was severely attenuated in IKKε-/- MEF infected with WNV, while induction of IFIT1 and IFIT3 expression remained comparable to wt controls (Fig. 1A). Furthermore, in absence of IKKε, we observed delayed and impaired IFIT2 expression following IFN-β stimulation, demonstrating that IKKε was important for IFIT2 induction in MEFs. In contrast, IFN-β stimulation efficiently induced the expression of IFIT1, IFIT3, and PKR regardless of IKKε expression (Fig. 1B). To further assess the specific role of IKKε in regulating ISG expression, we evaluated the ISG promoter-induction in HEK293 cells ectopically expressing IKKε. Ectopic overexpression of IKKε has been shown to induce its multimerization through the coiled-coil domain, causing its trans-autoactivation. Trans-autoactivation of IKKε results in its signaling to activate downstream substrates (such as IRF-3, IκBα, and AKT) and induce the expression of target genes (35-37). We found that ectopic expression of IKKε induced activation of *IFN*-β-promoter (which contains IRF-3, but not ISGF3 binding site) occurred in a dose-dependent manner, whereas treatment of cells with exogenous IFN-β did not induce promoter expression, as expected (Fig. 1C, $P < 0.0025$, *top-left panel*). Importantly, we observed a dose-dependent promoter activation of *ADAR1* and *IFIT2* (Fig. 1C, $P \leq 0.025$, *bottom panel*), but not *ISG15* upon IKKε ectopic expression (Fig. 1C, $P > 0.025$, *top-right panel*), further demonstrating the role of IKKε in induction of an ISG subset recently shown to be sensitive to IKKε and STAT1 S708 phosphorylation (21). Unlike ADAR1, whose promoter contains ISRE but not IRF-3 binding sites, the IFIT2 promoter contains both sites, each of which are IKKε responsive. Our results show that IKKε is essential for both virus-induced and IFN-induced IFIT2 expression,

Downloaded from www.jbc.org at NORTHWESTERN UNIV LIBRARY, on December 9, 2011

demonstrating dual roles of IKKε to induce innate effector ISG expression.

Since IFIT2 expression is induced by WNV infection, we assessed the antiviral actions of IFIT2 in restricting WNV-MAD infection in MEFs from wt and IFIT2-/- mice. Culture supernatants were collected at 0-, 6-, 24-, and 48-hours post infection, where time 0 represents input virus. Analysis of single-step virus growth revealed that WNV-MAD replication was enhanced in cells lacking IFIT2 compared to wt cells, thus validating IFIT2 function as a WNV restriction factor (Fig. 1D) (23). These results define IFIT2 as an IKKε-dependent ISG whose expression is induced by WNV infection and IFN-β to restrict WNV growth in primary cells.

Virus infection induces delayed STAT1 S708 phosphorylation– Since IFIT2 is induced by WNV infection in a manner dependent on IKKε; we sought to characterize the IKKε and STAT1 S708 phosphorylation kinetics in response to cell treatment with IFN-β. IKKε has previously shown to directly phosphorylate STAT1 S708 *in vitro* (21). We therefore generated novel phospho-specific, affinity-purified polyclonal antibody against a phosphorylated peptide representing phospho-STAT1 S708 (α-p-STAT1 S708; Fig. S2 A-C). We used this antibody to assess STAT1 S708 phosphorylation status after IFN-β-treatment, confirming that IKKε-/- MEFs were deficient in IFN-β-induced S708 STAT1 phosphorylation. In contrast, IFN-β-induced STAT1 Y701 and S727 phosphorylation occurred independently of IKKε (Fig. 2A). IKKε-mediated STAT1 S708 phosphorylation is independent of its role in IRF-3 activation, as activated IRF-3 efficiently translocated into the nucleus following SenV infection in absence of IKKε (Fig. S3). These results demonstrate the specificity of the α-p-STAT1 S708 antibody and confirm that IFN-induced STAT1 S708 phosphorylation is dependent on IKKε expression.

To further determine the kinetics of STAT1 S708 phosphorylation in response to RNA virus infection, we analyzed p-STAT1 S708 abundance during infection of HEK293 cells by the prototypic *Paramyxovirus,* Sendai virus (SenV), or WNV-MAD (Fig. 2B and 2C). Immunoblot analysis revealed that p-STAT1 S708 occurred at later time points during the infection cycle of either virus, happening between 18- to 24-hours post-infection with SenV and 72-hours post-infection with WNV-MAD. In both SenV and WNV infection models, phosphorylation of S708 appeared to be occurring much later than the canonical phosphorylation of STAT1 Y701, which began at 6-hours post-SenV infection and as early as 36-hours post-WNV infection. Moreover, phosphorylation of STAT Y701 was preceded by detectable levels of phosphorylated/activated IRF-3, which is consistent with endogenous IFN being expressed to drive IFNAR signaling of STAT1 phosphorylation (Fig. 2B). Together, these results demonstrate that both SenV and WNV-MAD infections stimulate STAT1 S708 phosphorylation late in the virus replication cycle, and that that IFIT2 expression associates with IFN-induced accumulation of p-STAT1 S708.

Type-I, type-II, and type-III IFNs induce STAT1 S708 phosphorylation– To determine if different classes of IFN stimulate STAT1 S708 phosphorylation, we compared the ability of type-I, -II, and -III IFNs to induce S708 phosphorylation in 2fTGH human fibrosarcoma cells after treatment with IFN-β (type-I IFN), IFN-γ (type-II IFN) or IFN-λ (type-III IFN). We found that IFN-β and IFN-γ treatment of cells induced STAT1 S708 phosphorylation after the onset of Y701 and S727 phosphorylation at late time post-treatment and similar to the kinetics of p-STAT1 S708 accumulation during WNV and SenV infection (Fig. 3A and 3B). In IFN-β-treated cells, STAT1 was immediately phosphorylated at Y701 and S727 within 10 and 30 minutes after treatment, respectively. In contrast, STAT1 S708 phosphorylation was first detectable at 16 hours and peaked at 24 hours post-treatment, which coincide with diminishing level of Y701 phosphorylation and expression of ADAR1 (like IFIT2, an IKKε-dependent ISG). Likewise, when treated with IFN-γ, 2fTGH cells induced STAT1 Y701 and S727 phosphorylation within 10 minutes and through 16 hours after treatment, while STAT1 S708 phosphorylation occurred at 16 hours post-treatment. To evaluate the ability of type-III IFN to stimulate STAT1 S708 phosphorylation, we examined the phosphorylation status of S708 in lysates of PH5CH8 cells, an immortalized hepatocyte cell line that expresses endogenous the type-III IFN receptor. Interestingly, we found that PH5CH8 cells treated with IFN-λ1 exhibited faster STAT1

Downloaded from www.jbc.org at NORTHWESTERN UNIV LIBRARY, on December 9, 2011

S708 phosphorylation kinetics compared to IFN-β treatment (Fig. 3C, lanes 5-7 and 10), with p-STAT1 S708 accumulating within 2 hours after IFN-λ1 treatment. In addition, we observed that p-STAT1 S727 was weakly phosphorylated following IFN-λ1 treatment compared to IFN-β. Furthermore, STAT1 Y701 phosphorylation was no longer sustained after 6 hours of IFN-λ1 treatment, a finding which contrasted with the phosphorylation kinetics observed in IFN-β-treated cells. In all cases, we found that IFN treatment induces phosphorylation of STAT1 at the Y701 residue before phosphorylation is detected on S708 (Fig. 3A-C). Together, these observations demonstrate that type-I, -II, and -III IFN are all able to induce STAT1 phosphorylation at residue S708, albeit with different kinetics.

Signaling through IFNAR is required for STAT1 S708 phosphorylation following type-I IFN treatment or virus infection – To evaluate the signaling requirements for WNV-MAD-induced STAT1 S708 phosphorylation, we infected wt, IRF-3-/-, and IFNAR-/- MEFs with WNV-MAD (MOI = 1) and analyzed STAT1 tyrosine and serine phosphorylation by immunoblot assay. As expected, phosphorylation of STAT1 at Y701 and S727 were ablated in the absence of IFNAR. Phosphorylation at S708 was similarly blocked despite the high abundance of phospho/active IRF-3 and IFN-β secretion of IFNAR-/- MEFs, indicating that active signaling through IFNAR is also required for STAT1 S708 phosphorylation during WNV-MAD infection (Fig. 4A, lanes 9-12; Fig. S4). Similarly, WNV-infected U5A human fibrosarcoma cells, which lack IFNAR2, also failed to induce STAT1 S708 phosphorylation compared to parental 2fTGH cells (Fig. 4B) (38). Next, we evaluate the IRF-3-signaling requirement for WNV-MAD-induced STAT1 S708 phosphorylation. In IRF-3-/- MEFs, there was a lack of STAT1 S708 phosphorylation during WNV-MAD infection (Fig. 4A, lanes 5-8), a finding that might be explained by the cellular defect in IFN-β production in the absence of IRF-3 (Fig. S4) (39). Thus, to assess the possible outcome due to loss of IFN-β production and its impact on p-STAT1 S708 accumulation in these cells, we compared p-STAT1 S708 abundance in wt, IRF-3-/-, and IFNAR-/- MEFs after treatment with 100 IU/ml IFN-β. p-STAT1 S708 levels in IRF-3-/- MEFs were similar or greater to the level found in wt MEFs after IFN-β treatment (Fig. 4C, lanes 3-4). However, IFN-β failed to induce STAT1 phosphorylation in IFNAR-/- MEFs and U5A cells (Fig. 4C, lanes 5-6; Fig. 4D). Thus, IFNAR signaling but not IRF-3 signaling is required for STAT1 S708 phosphorylation.

STAT1 S708 phosphorylation requires de novo protein synthesis– Because STAT1 S708 phosphorylation first requires IFN signaling, we sought to determine if an IFN-responsive factor(s) might be required to induce p-STAT1 S708 accumulation and the subsequent expression of IFIT2. To test this notion, we assessed p-STAT1 S708 abundance in 2fTGH cells that were either mock-treated or treated with cycloheximide-(CHX) for 30 minutes prior to a 16 hr IFN-β treatment time course. We observed that IFN-β-induced STAT1 phosphorylation at S708, but not Y701, is abrogated when *de novo* protein synthesis is blocked (Fig. 5A, lanes 6-10; Fig. S5A, lane 3). We found that when cells were pretreated with CHX for 16 hours and then subsequently treated with IFN-β for 1 hr, p-STAT1 Y701 still accumulated to high levels, revealing that available STAT1 molecules can be readily phosphorylated at Y701 during long term protein synthesis inhibition, and that IFN receptor signaling remains intact under these conditions. Thus, STAT1 phosphorylation on Y701 does not require *de novo* protein synthesis (Fig. 5A, lane 11). These observations also demonstrate that the CHX-treated cells were viable and responsive following 16-hours of protein synthesis inhibition (Fig. S5B). Similar to treatment with IFN-β, IFN-γ-induced accumulation of p-STAT1 S708, but neither Y701 nor S727 phosphorylation was also blocked in the presence of CHX (data not shown). Taken together, these data show that *de novo* protein synthesis is required for STAT1 S708 phosphorylation but not Y701 nor S727 phosphorylation following treatment of cells with IFN-β or IFN-γ. Thus, STAT1 S708 phosphorylation is induced and regulated though the actions of ISG product(s) whose expression precedes p-STAT1 S708 accumulation. Furthermore, we found that STAT1 S708 phosphorylation only occurred when CHX was added later than 9 hours after the addition of IFN-β (Fig. 5A, lanes 7-9), suggesting that the ISG product(s) required for STAT1 S708 phosphorylation is synthesized between 9- and 12-

Downloaded from www.jbc.org at NORTHWESTERN UNIV LIBRARY, on December 9, 2011

hours after the initiation of IFN-β treatment. In contrast, IFN-β stimulation of STAT1 Y701 phosphorylation occurred regardless of CHX treatment, indicating that the requirement for a *de novo* synthesized IFN-responsive gene product is specific to S708 phosphorylation (Fig. 5A, lane 6-11). Since STAT1 itself is an ISG, we assessed whether or not *de novo* STAT1 expression is required for S708 phosphorylation. We found that ectopic overexpression of STAT1 does not induce its phosphorylation at S708. Moreover, in the presence of IFN-β, we did not observe an acceleration of STAT1 S708 phosphorylation kinetics when compared to vector-transfected control cells (data not shown), demonstrating that *de novo* STAT1 expression does not immediately result in S708 phosphorylation. Thus, an IFN-responsive factor(s) but not STAT1 itself is the primary ISG product(s) driving STAT1 S708 phosphorylation and the IFN-induced expression IFIT2.

STAT1 S708 phosphorylation requires STAT1 tyrosine dephosphorylation and nuclear export – Given the different kinetics of STAT1 phosphorylation at various phospho-residues following IFN-β treatment, and the requirement for ISG expression to drive p-STAT1 S708 accumulation, we investigated whether the phosphorylation of STAT1 Y701 and S708 are linked. We assessed the impact of STAT1 Y701 phosphorylation on the accumulation of p-STAT1 S708 by pretreatment of cells to sustain STAT1 Y701 phosphorylation upon subsequent treatment with IFN-β. In the absence of inhibitor, IFN-β stimulation resulted in early induction of p-STAT1 Y701. However, p-STAT1 Y701 levels diminished after 16-hours of IFN-β stimulation despite increased total STAT1abundance (Fig. 5B, lane 1-3; Fig. 3A). Pretreatment of 2fTGH cells with CRM1 nuclear export inhibitor Leptomycin B (LMB) or protein tyrosine-phosphatase (PTP) inhibitor pervanadate for one hour before the start of IFN-treatment resulted in the sustained accumulation of p-STAT1 Y701 within IFN-treated cells (Fig. 5B, lane 4-9; (40-42)). In agreement with a previous report, pervanadate treatment of cells induced low level STAT1 activation in the absence of IFN-stimulation, and further enhanced STAT1 tyrosine phosphorylation following IFN-stimulation (Fig. 5B, lane 7-9; (42)). Importantly, there was an absence of p-STAT1 S708 concomitant with lack of IFN-induced ADAR1 expression [like IFIT2, an IKKε and p-STAT1 S708-dependent ISG (21)] in cells pretreated with either LMB (Fig. 5B, lane 4-6) or pervanadate (Fig. 5B, lane 7-9). However, STAT1 S727 phosphorylation and non-IKKε-dependent ISG expression were effectively induced upon IFN-β treatment of these cells. This observation suggests that STAT1 phosphorylation at Y701 and S708 residues are mutually exclusive, and removal of Y701 phosphorylation and subsequent STAT1 nuclear export are prerequisites the phosphorylation of STAT1 on S708.

To further assessed the relationship of p-STAT1 Y701 and S708, we evaluated STAT1 site-specific phosphorylation in STAT1-negative U3A cells reconstituted with transfected FLAG-tagged constructs containing either wt FLAG-STAT1, FLAG-STAT1 Y701E phosphomimetic, FLAG-Y701F phosphomutant, FLAG-S708A phosphomutant, FLAG-S708D phosphomimetic, FLAG-S727A phosphomutant, or a FLAG vector control. We assessed STAT1 phosphorylation at each site after cells were treated with IFN-β for 16 hr. We found that while STAT1 Y701 phosphorylation was absent in IFN-treated cells reconstituted with FLAG-STAT1 S708D, it was present in cells reconstituted with STAT1 S708A (Fig. S6, lane 6). Furthermore, we detected STAT1 S708 phosphorylation only in cells reconstituted with the FLAG-STAT1 Y701F or FLAG-STAT1 S708D, the latter observation defining the FLAG-STAT1 S708D construct as a direct phospho-mimetic recognized by our anti-phospho STAT1 S708 antibody. STAT1 S708 phosphorylation was not detected in cells expressing FLAG-STAT1 wt or FLAG-STAT1 S727A, both of which were phosphorylated on Y701 (Fig. S6, lane 2 and 7). In fact, we found that each of these constructs becomes immediately phosphorylated at Y701 upon IFN treatment and are sustained as such throughout the course of IFN-stimulation (data not shown). Cells reconstituted with FLAG-STAT1 Y701E failed to display S708 phosphorylation (Fig. S6, lane 3). Thus, p-STAT1 S708 likely takes place only after Y701 dephosphorylation and nuclear export, which occurs approximately at 16 hours post IFN-β stimulation.

IKKε mediates IFIT2 expression and protection against WNV pathogenesis in vivo – To

Downloaded from www.jbc.org at NORTHWESTERN UNIV LIBRARY, on December 9, 2011

determine the role of IKKε and STAT1 S708 phosphorylation in IFIT2 expression and protection against WNV infection *in vivo*, we examined the response of wt and IKKε-/- mice to WNV challenge. Wt and IKKε-/- mice were challenged with 10^3 pfu WNV-MAD by subcutaneous injection into the foot-pad. Clinical symptoms were monitored daily during the course of infection to observe the occurrence of disease and neurovirulence (12). When compared to the wt controls, IKKε-/- mice displayed earlier neurological symptoms, a higher degree of neurovirulence, and a failure to recover from acute WNV-MAD infection (Fig. 6A). Furthermore, we observed lack of sustained IFIT2 expression in the spleen of IKKε-/- mice during infection, and this associated with earlier virus entry to the spleen compared to wt controls (Fig. 6B). For comparison, we also challenged wt and IKKε-/- mice with the virulent/emergent lineage 1 Texas 02 strain of WNV (WNV-TX). This strain mediates a robust block to IFN signaling while evading the antiviral actions of IFIT2 (8;23). As expected, we observed similar but more rapid pathology defined by neurovirulence among wt and IKKε-/- mice infected with WNV-TX (data not shown). These observations reveal a dependence of IKKε for IFIT2 expression during WNV infection *in vivo*, and demonstrate that IKKε plays role in programming the innate immune response for the expression of IFIT2 and the control WNV infection. Our data also underscore the pathogenic outcome of WNV infection linked to viral evasion of IFN defenses.

DISCUSSION

Our study identifies IFIT2 as an innate immune effector gene that can restrict WNV replication, and defines the IKKε-mediated signaling pathway of IFN action that drives the expression of IFIT2 and a subset of ISGs through phosphorylation of STAT1 S708. Furthermore, we reveal that this IKKε pathway is dependent on an ISG product(s) to stimulate the IKKε-directed STAT-1 S708 phosphorylation at late times in the IFN response. Recent studies have demonstrated the importance of a variety of ISGs in controlling WNV infection, such as Viperin, IFITM2, IFITM3, ISG20, PKR, and IFIT2 (23;43). Moreover, The IFIT family members have been shown to suppress protein synthesis thus restricting replication of *Alphavirus*, *Papillomavirus*, and hepatitis C virus (28;44;45). Our results now show that IFIT2 can restrict WNV growth *in vitro* and demonstrate that its expression within an IKKε-dependent innate immune effector pathway associates with the control of virus spread and pathogenesis *in vivo*. Although the magnitude of the increase of WNV-MAD replication in IFIT2-/- cells was only ten-fold (one log), it is notable that this difference was statistically significant and caused by loss of a single ISG out of several hundred known ISGs, many of which might restrict WNV infection (43). These observations indicate the importance of IFIT2 in controlling growth of WNV, and indeed may in part explain the immune protection and lack of pathogencity after infection by low virulence WNV strains such as WNV-MAD and others, in animals (8;46;47).

IKKε has multiple roles in activating the innate immune response to virus infection, including the phosphorylation and activation of IRF-3, which leads to IFN-β production and phosphorylation of STAT1 at residue S708 following IFNAR signaling (21;48;49). The role of IKKε in STAT1 phosphorylation is independent on its role in IRF-3 activation, a role which is redundant with related kinase TBK1. MEFs lacking TBK1 are deficient in IRF-3 phosphorylation, indicating that TBK1 and not IKKε is the dominant kinase for IRF-3 activation, at least in MEFs (50). We conclude that IKKε functions to induce STAT1 S708 phosphorylation and a specific ISG expression signature that includes IFIT2 in WNV-infected cells. This conclusion is supported by our findings that ectopic overexpression of IKKε alone in human cells specifically stimulated *IFIT2* and *ADAR1* promoter induction whereas IFN-induced IFIT2 expression is strictly linked to STAT1 S708 phosphorylation and is dependent on IKKε *in vitro* and *in vivo* (see Fig. 1, 2 and 6) (21). Ectopic overexpression of a kinase such as IKKε induces its trans autoactivation facilitated by its multimerization, therefore bypassing the requirement for upstream signaling (35;36). In agreement with previous reports, IKKε overexpression also induces IFN-β promoter activation (Fig. 1C; (36)), suggesting general activation of IKKε target genes occurs upon its overexpression. However, IKKε expression alone

Downloaded from www.jbc.org at NORTHWESTERN UNIV LIBRARY, on December 9, 2011

did not induce the *ISG15* promoter, an ISG that can be induced through canonical ISGF3 function, which instead required IFN treatment (see Fig. 1). These data suggest that the expression of a specific ISG subset, that includes IFIT2, ADAR1 and others directly depends on IKKε, thus supporting the novel role for IKKε in antiviral immunity (21).

Our data now implicate this IKKε-dependent pathway and its specific expression of IFIT2 as important components of the innate immune response to WNV infection, and indicate that this response is governed by IKKε phosphorylation of STAT1 S708. IKKε-/- MEFs, which are deficient in STAT1 S708 phosphorylation, showed defects in IFN-induced IFIT2 expression, but not in other related ISGs including IFIT3 and IFIT1. We found that STAT1 S708 phosphorylation was induced by type-I, -II, and -III IFNs in addition to being induced during infection by WNV or SenV. Moreover, the kinetics of IFN-induced STAT1 S708 phosphorylation varied from phosphorylation at Y701 and S727. Whereas STAT1 Y701 and S727 phosphorylation occurred immediately following type-I and type-II IFN-stimulation as previously known (reviewed in (15)), S708 phosphorylation occurred later, at approximately 16 hours post-IFN treatment. In comparison, type-III IFN-induced phosphorylation of STAT1 S708 occurred more rapidly. This observation agrees with a previous report that demonstrated the differential kinetics and duration of JAK-STAT signaling activity induced by type-I and III IFN (51), and suggests that antiviral immune actions of these IFNs are each mediated in part through STAT1 S708-responsive ISGs. Similarly, STAT1 S708 phosphorylation was induced at later times following RNA virus infection, with delayed kinetics associated with WNV-MAD compared to SenV infection and likely due to the slower growth rate and IFN-induction of the former. These observations indicate that WNV and likely RNA virus infections in general indirectly stimulate STAT1 S708 phosphorylation via viral induction of IFN production from the infected cell, which then stimulates STAT1 S708 phosphorylation through the actions of IKKε.

We found that active signaling through the type-I IFN receptor was required for IFN-β- and virus-induced STAT1 S708 phosphorylation. IFN-induced STAT1 S708 phosphorylation, however, did not require IRF-3 expression. These observations are consistent with further data that IKKε-dependent IFIT2 induction can occur independently of IRF-3 (see Fig. 4C). However, during the course of virus infection, STAT1 S708 phosphorylation failed to take place in the absence of IRF-3 due to a lack of IFN-β induction, secretion, and signaling. Indeed, *de novo* protein synthesis downstream of IFN signaling was required for STAT1 S708 phosphorylation, suggesting that one or more ISG product signals IKKε to catalyze STAT1 S708 phosphorylation. This requirement of *de novo* IFN-induced factor synthesis for STAT1 S708-responsive ISG expression can be bypassed by IKKε overexpression which induces its autoactivation, suggesting that an IKKε activator ISG would function upstream of IKKε (see Fig. 1C). Although we have yet to determine the IFN-inducible factor that promotes S708 phosphorylation, based on CHX-pulse chase experiments, it appears to be synthesized between 9 and 12 hours after IFN-β stimulation. More detailed time course-dependent transcriptome profiling experiments may narrow down a list of candidate ISG that directly or indirectly in activating the kinase activity of IKKε that is responsible for S708 phosphorylation. Potential candidates could include the IFN-induced protein kinase PKR, which interacts with STAT1 without directly phosphorylating the Y701 residue (52) and restricts WNV infection in cells and *in vivo* (53;54), and p38, which has been implicated in ISRE activation following type-I IFN stimulation, but is not required for IFN-dependent STAT1 Y701 or S727 phosphorylation (55-57). Alternatively, protein phosphatases or non-enzymatic ISG products might be involved in modulating IKKε action and STAT1 S708 phosphorylation either through regulation of a signaling network of IKKε control or through direct binding to signaling factors of IKKε relevance or IKKε.

Our studies suggest that the order of STAT1 phosphorylation during the course of IFN stimulation could be an important contributor to the kinetics of ISG expression as STAT1 Y701 phosphorylation temporally precedes S708 phosphorylation and the induction of IFIT2 expression. Moreover, we observed minimal S708 phosphorylation in IFN-treated cells under

Downloaded from www.jbc.org at NORTHWESTERN UNIV LIBRARY, on December 9, 2011

conditions of pervanadate or LMB treatment, which blocks STAT1 tyrosine dephosphorylation and nuclear export, respectively (see Fig. 5B). Additionally, these treatments result in sustained Y701 phosphorylation of STAT1. These observations suggest that Y701 and S708 could be mutually exclusive on the same molecule. Consistent with this, STAT1 molecules that are phosphorylated at Y701 following IFN-β treatment are not phosphorylated on S708 (Fig. S6). These observations suggest one of two possible scenarios of STAT1 phosphorylation kinetics in which: (a) Y701 and S708 phosphorylation cannot occur simultaneously in a single STAT1 molecule whereas S727, which is more distantly located can; or (b) STAT1 molecules phosphorylated at Y701 cannot dimerize with STAT1 molecules phosphorylated at residue S708. We favor the former hypothesis due to the close proximity of Y701 and S708 residues, as phosphorylation at Y701 may result in steric hindrance of S708 phosphorylation. Importantly, we note that Y701 phosphorylation has been shown to diminish at later time points after IFN stimulation or virus infection due to nuclear STAT1 acetylation and dephosphorylation of Y701 by tyrosine phosphatase TCP45, which has been reported previously (40;58;59). Additionally, chromatin-bound STAT1 can be phosphorylated at S727 resulting in its sumoylation by UBC9 (60;61). As unphosphorylated STAT1 cycles back to the cytoplasm via CRM1-mediated nuclear export, acetylation and sumoylation results in STAT1 latency by inhibiting IFN-induced STAT1 Y701 phosphorylation, which should then permit S708 phosphorylation (58;59;61). These studies concluded that non-tyrosine phosphorylated STAT1 are the 'unphosphorylated STAT1', which functions to sustain expression of some ISGs (62;63). Our findings now suggest that the actual nature of these 'unphosphorylated STAT1' entities may be STAT1 phosphorylated at S708, thus promoting the expression of a specific subset of ISGs whose expression occurs later after IFN treatment, such as IFIT2, thus "sustaining" the IFN response. We therefore propose a model of early and late type-I IFN response programs (Fig. 7). Early after type-I IFN stimulation, STAT1 is phosphorylated at Y701, translocates to the nucleus, and induces expression of IKKε-independent ISGs. Following tyrosine dephosphorylation, STAT1 molecules are exported back to the cytoplasm. At a later time, as yet undetermined IFN-inducible factor(s) activate the IKKε-mediated STAT1 phosphorylation at S708 residue, which results in sustained expression of IKKε-dependent ISGs, including IFIT2. Similar to the actions of IFIT2 against WNV infection, we propose that IKKε-dependent ISGs include genes whose products direct antiviral and immune-modulatory actions to mediate innate immunity. Defining the nature of these ISGs within the innate immune response to WNV infection will be an important contribution toward identifying therapeutic targets for enhancement of immune protection against WNV and other flaviviruses. Therefore, genomics-based assessment of the response to WNV infection in wt and IKKε-/- mice, as well as targeted chromatin immunoprecipitation assay and analyses to define p-STAT1 S708-responsive genes is warranted for future studies aimed at characterizing this novel IKKε-dependent pathway of innate immunity.

The importance of IFIT2 and the IKKε pathway of ISG induction is underscored by the observation that virulent WNV effectively suppresses IFIT2 function to ensure efficient virus replication (23). Moreover, we have shown that a WNV strain that specifically lacks the ability to modulate the effect of IFIT genes is attenuated in wt mice (23;24;26). These observations, coupled with the present study showing that MEFs lacking IFIT2 support greater replication of WNV-MAD, a strain of WNV that only inefficiently antagonizes the antiviral effects of IFN (8), define IFIT2 as a innate immune effector gene that restricts WNV replication. Our studies also examined the significance of STAT1 S708 phosphorylation during the course of infection *in vivo*, through infection of IKKε-/- mice with WNV-MAD or WNV-TX, the latter being the emergent strain of WNV that is highly virulent and now circulates in North America (8). Whereas the WNV-MAD strain does not cause neurovirulence in adult wt C57BL/6 mice, the WNV-TX strain is highly neurovirulent (8;64). Importantly, in isogenic IKKε-/- mice, WNV-MAD disseminated to the spleen at earlier times and caused increased clinical disease, although none of the animals succumbed to lethal infection over the study time course. Furthermore, IFIT2 expression was not

Downloaded from www.jbc.org at NORTHWESTERN UNIV LIBRARY, on December 9, 2011

sustained in the spleen of these animals at later time during WNV-MAD infection. However, early IFIT2 induction likely resulted from IRF-3 activation, as IFIT2 is responsive to both IRF-3 and IFN-stimulation which can be differentially regulated in different cell types of the spleen. These studies confirmed the IKKε-dependency for STAT1 S708 phosphorylation and sustained IFIT2 expression during virus infection to demonstrate a role for the IKKε pathway of IFIT2 expression *in vivo* during WNV infection (see Fig. 6). Viral suppression of IFIT2 or IKKε signaling may therefore impart replication fitness for the support of viral spread and tissue dissemination and therefore represents a virulence determinant among strains of WNV and possibly other pathogenic viruses. The IKKε pathway could therefore prove attractive for therapeutic strategies aimed at limiting virus replication and enhancing innate antiviral immunity. Further work to define this pathway will reveal the nature of IKKε signaling control during the response to IFN.

REFERENCES

1. Lanciotti, R. S., Roehrig, J. T., Deubel, V., Smith, J., Parker, M., Steele, K., Crise, B., Volpe, K. E., Crabtree, M. B., Scherret, J. H., Hall, R. A., MacKenzie, J. S., Cropp, C. B., Panigrahy, B., Ostlund, E., Schmitt, B., Malkinson, M., Banet, C., Weissman, J., Komar, N., Savage, H. M., Stone, W., McNamara, T., and Gubler, D. J. (1999) *Science* **286,** 2333-2337
2. Smithburn, K. C., Hughes, T. P., Burke, A. W., and Paul, J. H. (1940) *J.Trop.Med.Hyg.* **20,** 471-492
3. Berthet, F. X., Zeller, H. G., Drouet, M. T., Rauzier, J., Digoutte, J. P., and Deubel, V. (1997) *J.Gen.Virol.* **78 (Pt 9),** 2293-2297
4. Lanciotti, R. S., Ebel, G. D., Deubel, V., Kerst, A. J., Murri, S., Meyer, R., Bowen, M., McKinney, N., Morrill, W. E., Crabtree, M. B., Kramer, L. D., and Roehrig, J. T. (2002) *Virology* **298,** 96-105
5. Lvov, D. K., Butenko, A. M., Gromashevsky, V. L., Kovtunov, A. I., Prilipov, A. G., Kinney, R., Aristova, V. A., Dzharkenov, A. F., Samokhvalov, E. I., Savage, H. M., Shchelkanov, M. Y., Galkina, I. V., Deryabin, P. G., Gubler, D. J., Kulikova, L. N., Alkhovsky, S. K., Moskvina, T. M., Zlobina, L. V., Sadykova, G. K., Shatalov, A. G., Lvov, D. N., Usachev, V. E., and Voronina, A. G. (2004) *Arch.Virol.Suppl* 85-96
6. Jia, X. Y., Briese, T., Jordan, I., Rambaut, A., Chi, H. C., MacKenzie, J. S., Hall, R. A., Scherret, J., and Lipkin, W. I. (1999) *Lancet* **354,** 1971-1972
7. Daffis, S., Samuel, M. A., Suthar, M. S., Keller, B. C., Gale, M., Jr., and Diamond, M. S. (2008) *J.Virol.* **82,** 8465-8475
8. Keller, B. C., Fredericksen, B. L., Samuel, M. A., Mock, R. E., Mason, P. W., Diamond, M. S., and Gale, M., Jr. (2006) *J.Virol.* **80,** 9424-9434
9. Keller, B. C., Johnson, C. L., Erickson, A. K., and Gale, M., Jr. (2007) *Cytokine Growth Factor Rev.* **18,** 535-544
10. Fredericksen, B. L., Keller, B. C., Fornek, J., Katze, M. G., and Gale, M., Jr. (2008) *J.Virol.* **82,** 609-616
11. Loo, Y. M., Fornek, J., Crochet, N., Bajwa, G., Perwitasari, O., Martinez-Sobrido, L., Akira, S., Gill, M. A., Garcia-Sastre, A., Katze, M. G., and Gale, M., Jr. (2008) *J.Virol.* **82,** 335-345
12. Suthar, M. S., Ma, D. Y., Thomas, S., Lund, J. M., Zhang, N., Daffis, S., Rudensky, A. Y., Bevan, M. J., Clark, E. A., Kaja, M. K., Diamond, M. S., and Gale, M., Jr. (2010) *PLoS.Pathog.* **6,** e1000757
13. Gale, M., Jr. and Foy, E. M. (2005) *Nature* **436,** 939-945
14. Saito, T. and Gale, M., Jr. (2007) *Curr.Opin.Immunol.* **19,** 17-23
15. Darnell, J. E., Jr., Kerr, I. M., and Stark, G. R. (1994) *Science* **264,** 1415-1421
16. Hengel, H., Koszinowski, U. H., and Conzelmann, K. K. (2005) *Trends Immunol.* **26,** 396-401
17. Levy, D. E. and Garcia-Sastre, A. (2001) *Cytokine Growth Factor Rev.* **12,** 143-156
18. Sen, G. C. (2001) *Annu.Rev.Microbiol.* **55,** 255-281
19. Uddin, S., Sassano, A., Deb, D. K., Verma, A., Majchrzak, B., Rahman, A., Malik, A. B., Fish, E. N., and Platanias, L. C. (2002) *J.Biol.Chem.* **277,** 14408-14416
20. Varinou, L., Ramsauer, K., Karaghiosoff, M., Kolbe, T., Pfeffer, K., Muller, M., and Decker, T. (2003) *Immunity.* **19,** 793-802

Downloaded from www.jbc.org at NORTHWESTERN UNIV LIBRARY, on December 9, 2011

21. Tenoever, B. R., Ng, S. L., Chua, M. A., McWhirter, S. M., Garcia-Sastre, A., and Maniatis, T. (2007) *Science* **315,** 1274-1278
22. Platanias, L. C. (2005) *Nat.Rev.Immunol.* **5,** 375-386
23. Daffis, S., Szretter, K. J., Schriewer, J., Li, J., Youn, S., Errett, J., Lin, T. Y., Schneller, S., Zust, R., Dong, H., Thiel, V., Sen, G. C., Fensterl, V., Klimstra, W. B., Pierson, T. C., Buller, R. M., Gale, M., Jr., Shi, P. Y., and Diamond, M. S. (2010) *Nature* **468,** 452-456
24. Fensterl, V. and Sen, G. C. (2010) *J Interferon Cytokine Res*
25. Sarkar, S. N. and Sen, G. C. (2004) *Pharmacol.Ther.* **103,** 245-259
26. Terenzi, F., Hui, D. J., Merrick, W. C., and Sen, G. C. (2006) *J Biol.Chem.* **281,** 34064-34071
27. Hui, D. J., Terenzi, F., Merrick, W. C., and Sen, G. C. (2005) *J Biol.Chem.* **280,** 3433-3440
28. Wang, C., Pflugheber, J., Sumpter, R., Jr., Sodora, D. L., Hui, D., Sen, G. C., and Gale, M., Jr. (2003) *J Virol.* **77,** 3898-3912
29. Daffis, S., Samuel, M. A., Keller, B. C., Gale, M., Jr., and Diamond, M. S. (2007) *PLoS.Pathog.* **3,** e106
30. Bluyssen, H. A., Vlietstra, R. J., Faber, P. W., Smit, E. M., Hagemeijer, A., and Trapman, J. (1994) *Genomics* **24,** 137-148
31. Bandyopadhyay, S. K., Leonard, G. T., Jr., Bandyopadhyay, T., Stark, G. R., and Sen, G. C. (1995) *J Biol.Chem.* **270,** 19624-19629
32. Wacher, C., Muller, M., Hofer, M. J., Getts, D. R., Zabaras, R., Ousman, S. S., Terenzi, F., Sen, G. C., King, N. J., and Campbell, I. L. (2007) *J Virol.* **81,** 860-871
33. Hemmi, H., Takeuchi, O., Sato, S., Yamamoto, M., Kaisho, T., Sanjo, H., Kawai, T., Hoshino, K., Takeda, K., and Akira, S. (2004) *J.Exp.Med.* **199,** 1641-1650
34. Foy, E., Li, K., Wang, C., Sumpter, R., Jr., Ikeda, M., Lemon, S. M., and Gale, M., Jr. (2003) *Science* **300,** 1145-1148
35. Peters, R. T., Liao, S. M., and Maniatis, T. (2000) *Molecular Cell* **5,** 513-522
36. Breiman, A., Grandvaux, N., Lin, R., Ottone, C., Akira, S., Yoneyama, M., Fujita, T., Hiscott, J., and Meurs, E. F. (2005) *J.Virol.* **79,** 3969-3978
37. Xie, X., Zhang, D., Zhao, B., Lu, M. K., You, M., Condorelli, G., Wang, C. Y., and Guan, K. L. (2011) *Proceedings of the National Academy of Sciences* **108,** 6474-6479
38. Pellegrini, S., John, J., Shearer, M., Kerr, I. M., and Stark, G. R. (1989) *Mol.Cell Biol.* **9,** 4605-4612
39. Sato, M., Suemori, H., Hata, N., Asagiri, M., Ogasawara, K., Nakao, K., Nakaya, T., Katsuki, M., Noguchi, S., Tanaka, N., and Taniguchi, T. (2000) *Immunity.* **13,** 539-548
40. Haspel, R. L., Salditt-Georgieff, M., and Darnell, J. E., Jr. (1996) *EMBO J* **15,** 6262-6268
41. McBride, K. M. and Reich, N. C. (2003) *Sci.STKE.* **2003,** RE13
42. Mowen, K. and David, M. (2000) *Mol.Cell Biol.* **20,** 7273-7281
43. Jiang, D., Weidner, J. M., Qing, M., Pan, X. B., Guo, H., Xu, C., Zhang, X., Birk, A., Chang, J., Shi, P. Y., Block, T. M., and Guo, J. T. (2010) *J Virol.* **84,** 8332-8341
44. Zhang, Y., Burke, C. W., Ryman, K. D., and Klimstra, W. B. (2007) *J Virol.* **81,** 11246-11255
45. Terenzi, F., Saikia, P., and Sen, G. C. (2008) *EMBO J* **27,** 3311-3321
46. Daffis, S., Suthar, M. S., Gale, M., Jr., and Diamond, M. S. (2009) *J Innate.Immun.* **1,** 435-445
47. Daffis, S., Lazear, H. M., Liu, W. J., Audsley, M., Engle, M., Khromykh, A. A., and Diamond, M. S. (2011) *J Virol.* **85,** 5664-5668
48. Fitzgerald, K. A., McWhirter, S. M., Faia, K. L., Rowe, D. C., Latz, E., Golenbock, D. T., Coyle, A. J., Liao, S. M., and Maniatis, T. (2003) *Nat.Immunol.* **4,** 491-496
49. Tenoever, B. R., Sharma, S., Zou, W., Sun, Q., Grandvaux, N., Julkunen, I., Hemmi, H., Yamamoto, M., Akira, S., Yeh, W. C., Lin, R., and Hiscott, J. (2004) *J.Virol.* **78,** 10636-10649
50. McWhirter, S. M., Fitzgerald, K. A., Rosains, J., Rowe, D. C., Golenbock, D. T., and Maniatis, T. (2004) *Proc.Natl.Acad.Sci.U.S.A* **101,** 233-238
51. Maher, S. G., Sheikh, F., Scarzello, A. J., Romero-Weaver, A. L., Baker, D. P., Donnelly, R. P., and Gamero, A. M. (2008) *Cancer Biol.Ther.* **7,** 1109-1115

Downloaded from www.jbc.org at NORTHWESTERN UNIV LIBRARY, on December 9, 2011

52. Wong, A. H.-T., Tam, N. W. N., Yang, Y. L., Cuddihy, A. R., Li, S., Kirchhoff, S., Hauser, H., Decker, T., and Koromilas, A. E. (1997) *EMBO J* **16,** 1291-1304
53. Samuel, M. A., Whitby, K., Keller, B. C., Marri, A., Barchet, W., Williams, B. R., Silverman, R. H., Gale, M., Jr., and Diamond, M. S. (2006) *J.Virol.* **80,** 7009-7019
54. Gilfoy, F. D. and Mason, P. W. (2007) *J Virol.* **81,** 11148-11158
55. Katsoulidis, E., Li, Y., Mears, H., and Platanias, L. C. (2005) *J.Interferon Cytokine Res.* **25,** 749-756
56. Uddin, S., Lekmine, F., Sharma, N., Majchrzak, B., Mayer, I., Young, P. R., Bokoch, G. M., Fish, E. N., and Platanias, L. C. (2000) *J.Biol.Chem.* **275,** 27634-27640
57. Uddin, S., Majchrzak, B., Woodson, J., Arunkumar, P., Alsayed, Y., Pine, R., Young, P. R., Fish, E. N., and Platanias, L. C. (1999) *J.Biol.Chem.* **274,** 30127-30131
58. Kramer, O. H., Knauer, S. K., Greiner, G., Jandt, E., Reichardt, S., Guhrs, K. H., Stauber, R. H., Bohmer, F. D., and Heinzel, T. (2009) *Genes Dev.* **23,** 223-235
59. Kramer, O. H. and Heinzel, T. (2010) *Mol.Cell Endocrinol.* **315,** 40-48
60. Vanhatupa, S., Ungureanu, D., Paakkunainen, M., and Silvennoinen, O. (2008) *Biochem J* **409,** 179-185
61. Zimnik, S., Gaestel, M., and Niedenthal, R. (2009) *Nucleic Acids Res* **37,** e30
62. Cheon, H. and Stark, G. R. (2009) *Proc.Natl.Acad.Sci.U.S.A* **106,** 9373-9378
63. Yang, J. and Stark, G. R. (2008) *Cell Res* **18,** 443-451
64. Beasley, D. W. C., Li, L., Suderman, M. T., and Barrett, A. D. T. (2002) *Virology* **296,** 17-23

Abbreviations

ADAR, double-stranded RNA-specific adenosine deaminase; hpi, hours post infection; IFIT, IFN-induced protein with tetratricopeptide repeats; IKK, IκB kinase; IRF, interferon regulatory factor; ISG, interferon-stimulated gene; ISRE, interferon- stimulated regulatory element; IU, international unit; JAK, Janus kinase; MDA5, melanoma differentiation-associated protein 5; PKR, protein kinase R; PRR, pattern recognition receptor; RIG-I, retinoic-inducible gene-I; SenV, Sendai virus; TBK, TRAF family member associated NF-κB activator (TANK)-binding kinase 1; Tyk, tyrosine kinase; WNV, West Nile virus.

Acknowledgements

This work was supported by NIH grants R01AI074973 and U19AI083019. We would like to thank Drs. Stacy Horner, Yueh Ming-Loo, Courtney Wilkins, Helene Liu, and Renee Ireton for critical reading of the manuscript, and Arjun Rustagi for the generation of IRF-3 antibody.

Figure Legends

FIGURE 1. IKKε and IFIT2 impose restriction of WNV infection. Wt or IKKε-/- MEFs were **(A)** mock-infected or infected with WNV-MAD at an MOI of 1, and **(B)** mock-stimulated or stimulated with 100 IU/ml IFN-β. Protein lysate was collected at indicated times and immunoblotted using IFIT2, IFIT3, IFIT1, PKR, and IKKε antibodies. Tubulin was used as loading control. **(C)** HEK293 cells were co-transfected with pCMV-Renilla and either pIFN-β-Luciferase (top-left), pISG15-Luciferase (top-right), pADAR1-Luciferase (bottom-left), or pIFIT2-Luciferase (bottom-right). 16 hours later, cells were either mock-stimulated (vector co-transfection), stimulated by transfection with 25ng, 50ng, or 100ng of an IKKε expression plasmid, or treated with 100 IU/ml IFN-β. Cells were harvested 48 hours post-transfection and luciferase expression was measured and normalized to Renilla. Relative Luciferase value was calculated as fold induction over induction of vector that was set to 1. Statistical analysis was performed with Student's t test. **(D)** Wt or IFIT2-/- MEFs were infected with WNV-MAD at an MOI of 5. At the indicated time points post-infection, culture supernatants were collected and virus titers were determined by plaque assay on BHK cells. **(C-D)** The data is the average of three independent experiments performed in triplicate and error bars represent standard deviation. P-values were calculated using student's t-test to determine statistical significance.

Downloaded from www.jbc.org at NORTHWESTERN UNIV LIBRARY, on December 9, 2011

FIGURE 2. Virus infection induces delayed STAT1 S708 phosphorylation. **(A)** Wt or IKKε-/- MEFs were mock-stimulated or stimulated with 100IU/ml IFN-β. Protein lysate was collected 16 hours post-IFN-stimulation immunoblotted using p-STAT1 S708, p-STAT1 S727, p-STAT1 Y701, and total STAT1 antibodies. **(B & C)** Sendai and WNV virus infections induce STAT1 S708 phosphorylation. HEK293 cells were infected with **(B)** 100 HA U/ml Sendai virus (SenV) or **(C)** West Nile virus strain Madagascar (WNV-MAD) at an MOI of 1. At the indicated times following infection, protein lysates were collected and immunoblotted for p-STAT1 S708, p-STAT1 Y701, total STAT1, p-IRF-3, total IRF-3, IFIT1, and SenV or WNV. Tubulin and GAPDH were used as loading controls.

FIGURE 3. Type-I, type-II, and type-III IFNs induce STAT1 S708 phosphorylation. 2fTGH cells were mock-treated or treated with **(A)** 100IU/ml IFN-β or **(B)** 50ng/ml IFN-γ. **(C)** PH5CH8 cells were mock-treated (lane 1), treated with 100ng/ml IFN-λ1 (lane 2-6), or 100IU/ml of IFN-β (lane 7-9). Protein lysate was collected at respective time points following IFN treatment and immunoblotted for p-STAT1 S708 , p-STAT1 Y701, p-STAT1 S727, total STAT1, ADAR1, and IFIT1.

FIGURE 4. Signaling through IFNAR is required for STAT1 S708 phosphorylation following type-I IFN treatment or virus infection. **(A)** wt, IRF-3-/-, or IFNAR-/-, and **(B)** parental 2fTGH cells or their derivative U5A cells (which lack IFNAR) were infected with WNV-MAD at an MOI of 1. Protein lysates were collected at the indicated time points and immunoblotted for p-STAT1 S708 , p-STAT1 Y701, p-STAT1 S727, total STAT1, p-IRF-3, total IRF-3, and WNV. **(C, D)** The same cells were also mock-stimulated or stimulated with 100IU/ml IFN-β for 6 or 16 hours. Protein lysates were collected at the indicated time points and immunoblotted for p-STAT1 S708 , p-STAT1 Y701, p-STAT1 S727, total STAT1, p-IRF-3, total IRF-3, IFIT2, IFIT3, and IFIT1. (*, non specific band)

FIGURE 5. STAT1 S708 phosphorylation requires de novo protein synthesis, STAT1 tyrosine dephosphorylation, and nuclear export. **(A)** 2fTGH cells were mock-treated (-CHX, lane 1-5) or treated with CHX (+CHX, lane 6-11) to block protein synthesis. At 30 minutes (lane 6-10) or 16 hours (lane 11) following CHX treatment, cells were mock-stimulated (M) or stimulated with IFN-β. Cells were harvested at 10 minutes as well as 1, 6, and 16 hours post-IFN stimulation and immunoblotted to detect p-STAT1 S708, p-STAT1 Y701, total STAT1, ISG15, and IFIT1. **(B)** 2fTGH cells were non-treated (NT; lane 1-3), pretreated with 100nM of Leptomycin B (LMB; lane 4-6), or 50mM pervanadate (Van; lane 7-9) one hour before mock-stimulation (M) or stimulation with 100 IU/ml IFN-β. Cells were harvested at 1- and 16- hours post-stimulation. Immunoblot analysis was performed using p-STAT1 S708, p-STAT1 Y701, p-STAT1 S727, total STAT1, ADAR1, and IFIT1 antibodies.

FIGURE 6. IKKε mediates IFIT2 expression and protection against WNV pathogenesis *in vivo*. Wt Bl6 and IKKε-/- mice were mock-infected (PBS-only) or infected with 10^3 pfu of WNV-MAD subcutaneously through foot pad injection. **(A)** Mice were monitored and scored daily for clinical symptoms over 17 days. Clinical scores from four representative mice per group were graphed. **(B)** Spleens from wt or IKKε-/- mice, mock infected or infected with WNV-MAD, were collected at day 4-, 6-, and 12-post infection. Protein lysates were extracted by homogenizing spleens with RIPA and immunoblotted using p-STAT1 S708, p-STAT1 Y701, p-STAT1 S727, total STAT1, IFIT2, IFIT1, WNV, and IKKε antibodies. Immunoblot panel is a representative from four mice per infection group.

FIGURE 7. A model illustrating that early and late ISGs induction is regulated by multiple STAT1 post-translational modifications. 1) The canonical JAK-STAT signaling is activated following type-I IFN binding to its receptor which results in STAT1 Y701 phosphorylation, ISGF3 formation, and its nuclear translocation. ISGF3 binding to ISRE element induces transcription of ISGs. 2) Chromatin-bound STAT1 can be phosphorylated by MAPK at residue S727 which induces its sumoylation. 3-4) Nuclear STAT1 is also acetylated by HAT CBP resulting in recruitment of TCP1 which catalyze STAT1 tyrosine-

Downloaded from www.jbc.org at NORTHWESTERN UNIV LIBRARY, on December 9, 2011

dephosphorylation. Sumoylated-acetylated STAT1 cycles back to cytoplasm and both modifications render STAT1 unable to be further tyrosine-phosphorylated. 5-6) Type-I IFN signaling and unknown IFN-stimulated factor(s) activate IKKε phosphorylation of STAT1 S708. 7) STAT1 molecules phosphorylated at S708 can enter nucleus and induce expression of specific ISG subset (pY, tyrosine phosphorylation; pS, serine phosphorylation, Ac, acetylation; Su, sumoylation).

Downloaded from www.jbc.org at NORTHWESTERN UNIV LIBRARY, on December 9, 2011

Figure 1

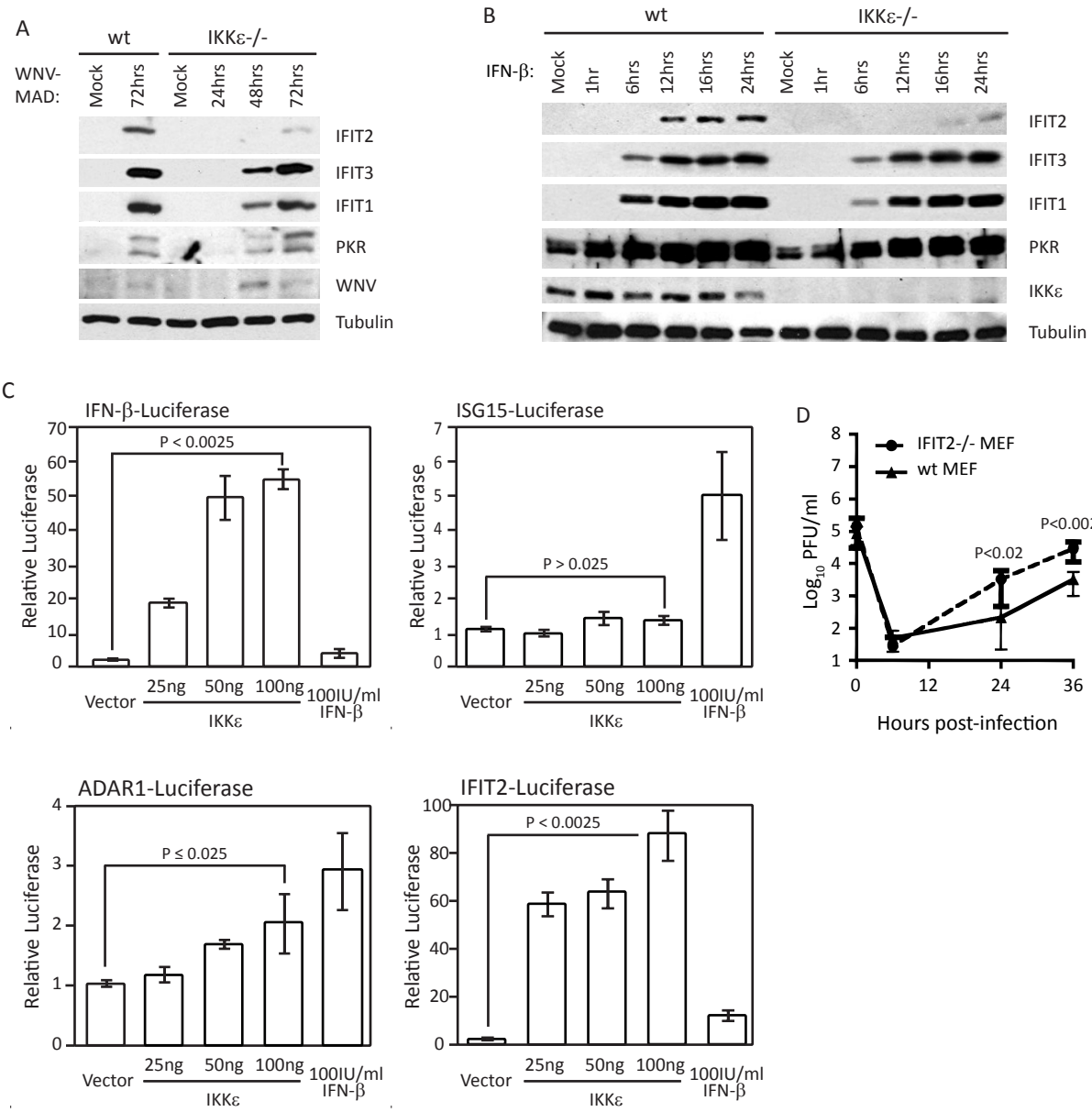

Downloaded from www.jbc.org at NORTHWESTERN UNIV LIBRARY, on December 9, 2011

Figure 2

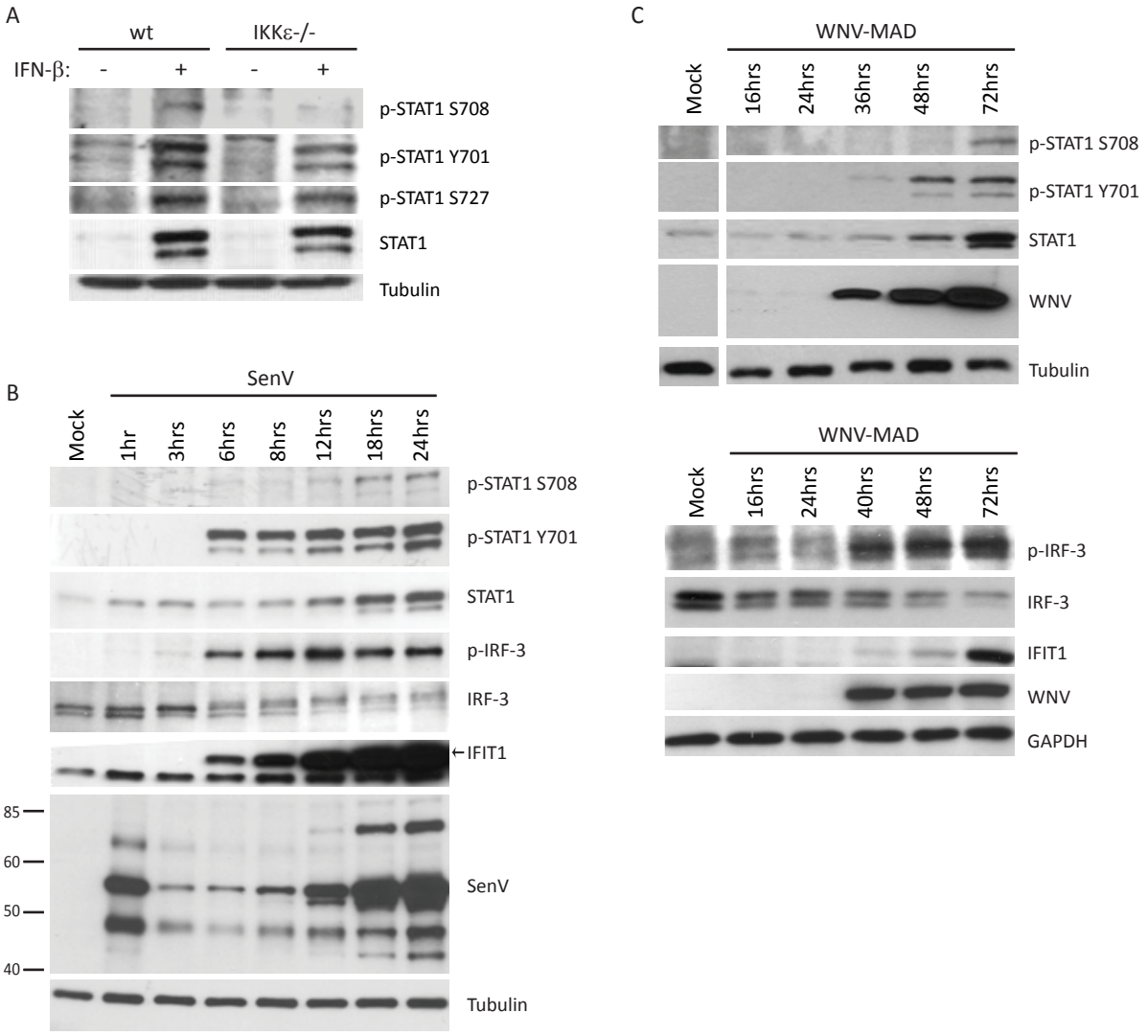

Downloaded from www.jbc.org at NORTHWESTERN UNIV LIBRARY, on December 9, 2011

Figure 3

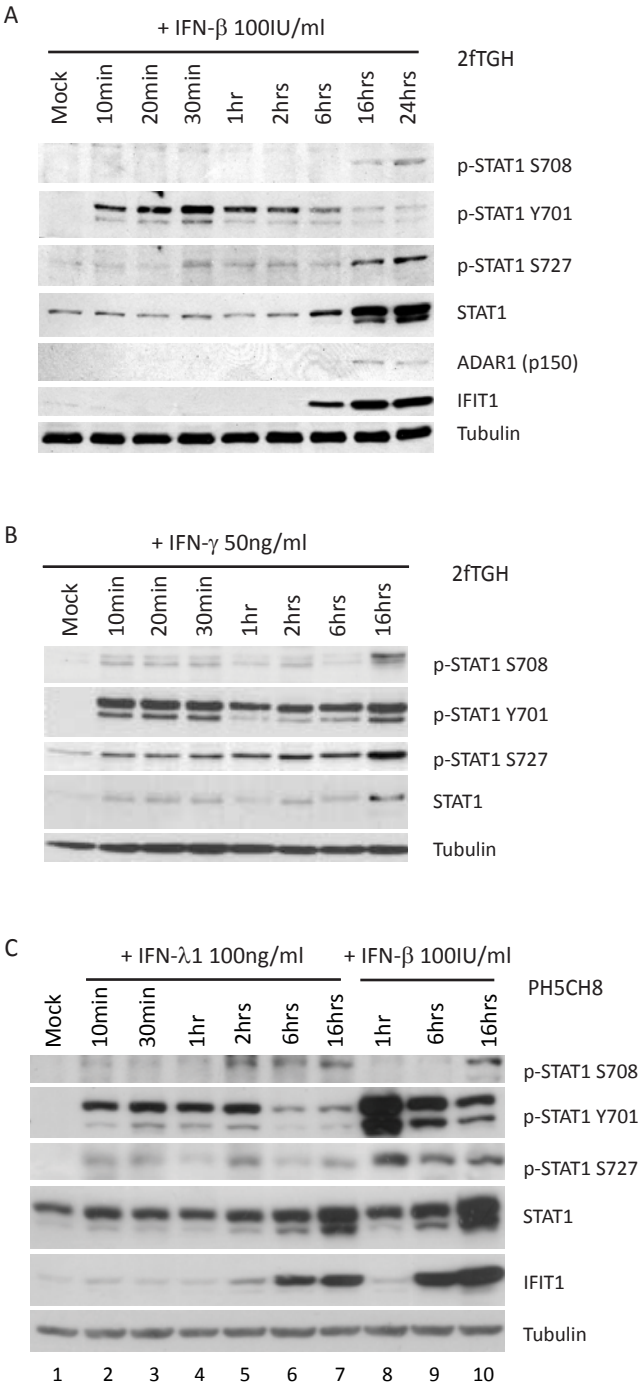

Downloaded from www.jbc.org at NORTHWESTERN UNIV LIBRARY, on December 9, 2011

Figure 4

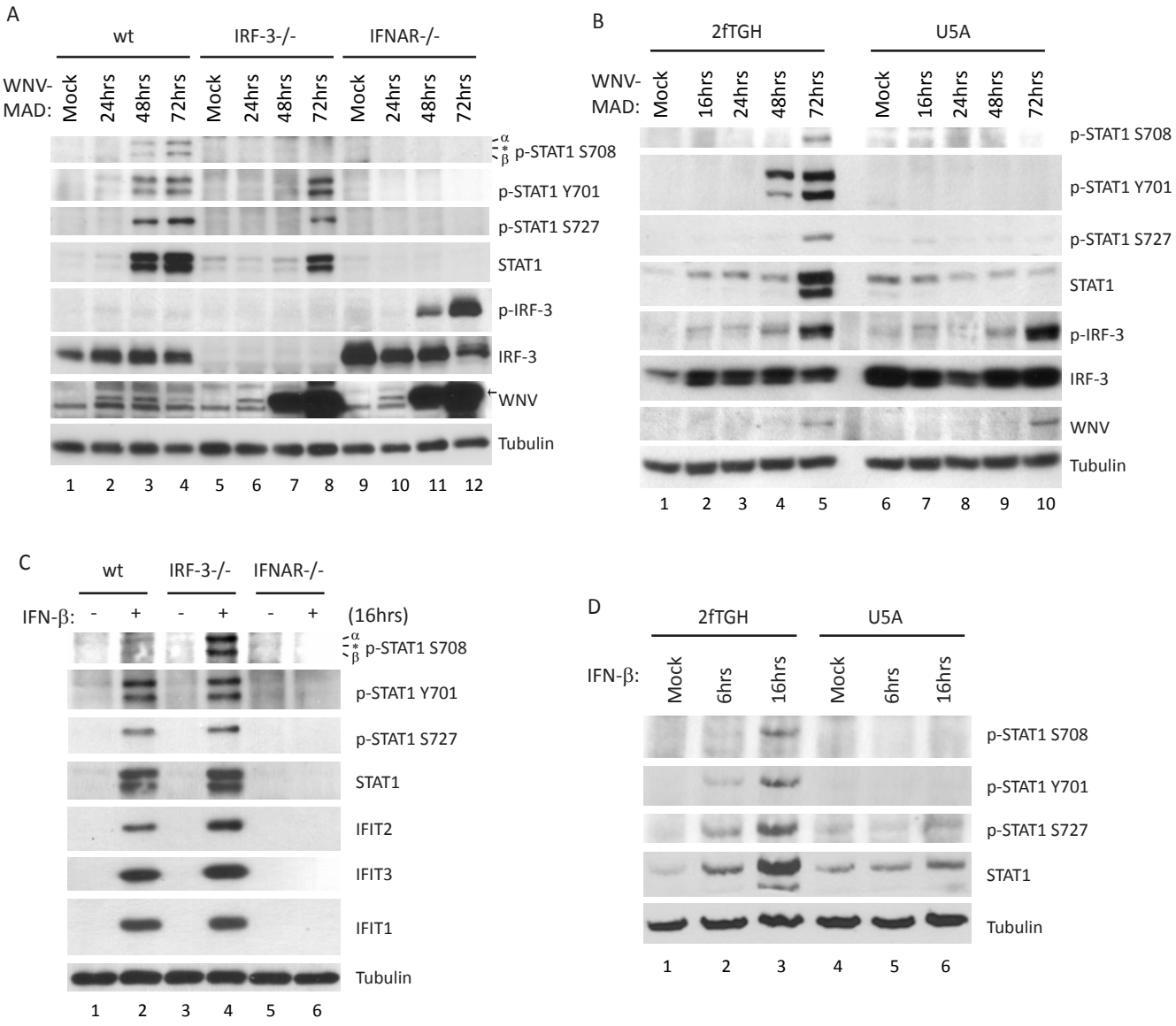

Downloaded from www.jbc.org at NORTHWESTERN UNIV LIBRARY, on December 9, 2011

Figure 5

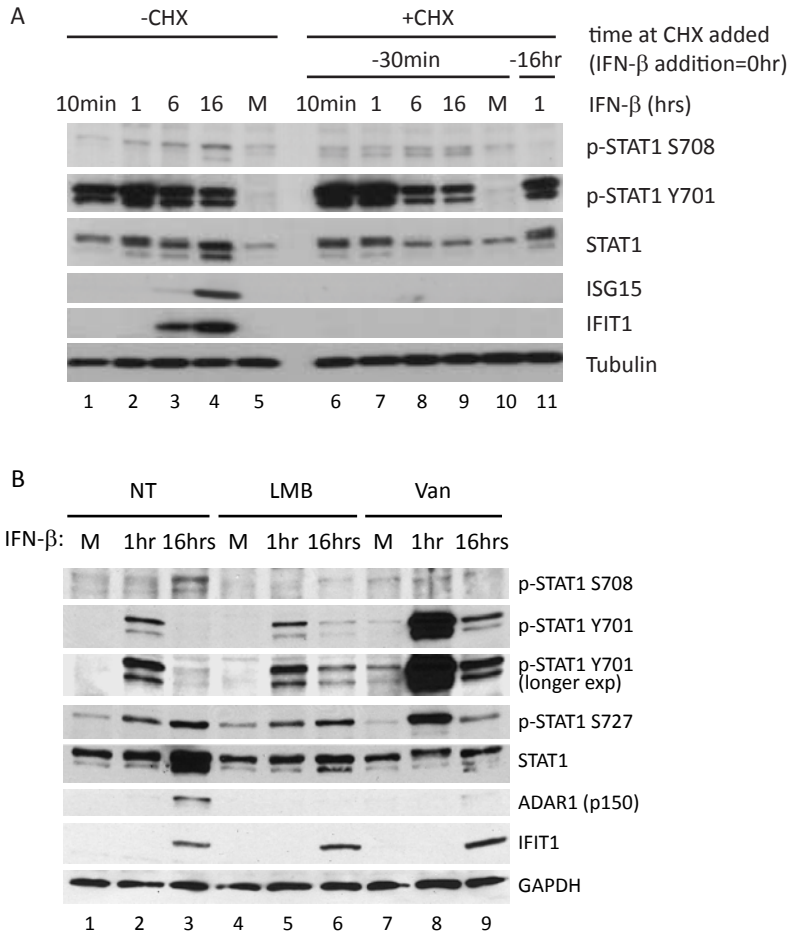

Downloaded from www.jbc.org at NORTHWESTERN UNIV LIBRARY, on December 9, 2011

Figure 6

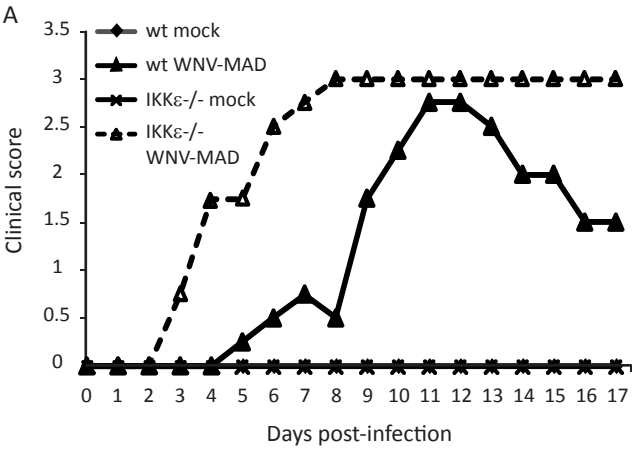

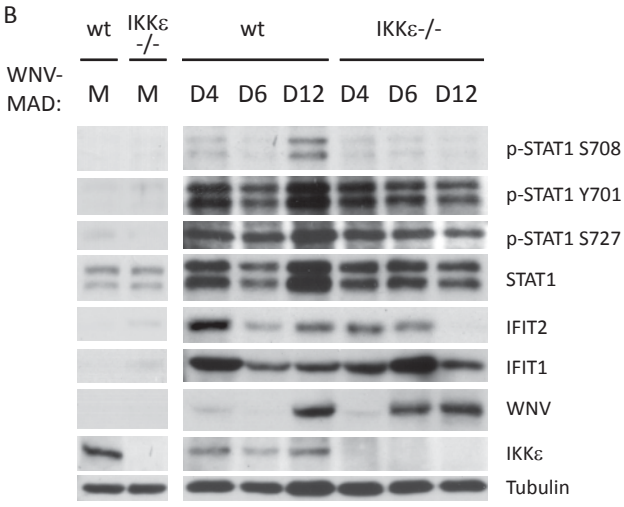

Downloaded from www.jbc.org at NORTHWESTERN UNIV LIBRARY, on December 9, 2011

Figure 7

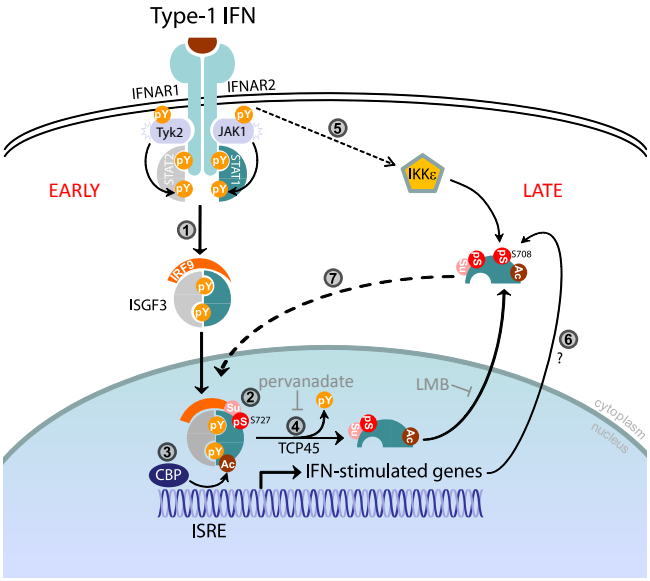

Downloaded from www.jbc.org at NORTHWESTERN UNIV LIBRARY, on December 9, 2011

Cell Host & Microbe
Article

Conserved Herpesvirus Kinases Target the DNA Damage Response Pathway and TIP60 Histone Acetyltransferase to Promote Virus Replication

Renfeng Li,[1,7] Jian Zhu,[2,3,7] Zhi Xie,[4] Gangling Liao,[1] Jianyong Liu,[1] Mei-Ru Chen,[6] Shaohui Hu,[2,3] Crystal Woodard,[2,3] Jimmy Lin,[1] Sean D. Taverna,[2] Prashant Desai,[1,5] Richard F. Ambinder,[1,5] Gary S. Hayward,[1,2,5] Jiang Qian,[1,4,5] Heng Zhu,[1,2,3,5,*] and S. Diane Hayward[1,2,5,*]
[1]Department of Oncology
[2]Department of Pharmacology and Molecular Sciences
[3]High Throughput Biology Center
[4]Department of Opthalmology
Johns Hopkins School of Medicine, Baltimore, MD 21231, USA
[5]Kimmel Cancer Center, Baltimore, MD, 21231, USA
[6]Graduate Institute and Department of Microbiology, College of Medicine, National Taiwan University, Taipei 10617, Taiwan
[7]These authors contributed equally to this work
*Correspondence: heng.zhu@jhmi.edu (H.Z.), dhayward@jhmi.edu (S.D.H.)
DOI 10.1016/j.chom.2011.08.013

SUMMARY

Herpesviruses, which are major human pathogens, establish life-long persistent infections. Although the α, β, and γ herpesviruses infect different tissues and cause distinct diseases, they each encode a conserved serine/threonine kinase that is critical for virus replication and spread. The extent of substrate conservation and the key common cell-signaling pathways targeted by these kinases are unknown. Using a human protein microarray high-throughput approach, we identify shared substrates of the conserved kinases from herpes simplex virus, human cytomegalovirus, Epstein-Barr virus (EBV), and Kaposi's sarcoma-associated herpesvirus. DNA damage response (DDR) proteins were statistically enriched, and the histone acetyltransferase TIP60, an upstream regulator of the DDR pathway, was required for efficient herpesvirus replication. During EBV replication, TIP60 activation by the BGLF4 kinase triggers EBV-induced DDR and also mediates induction of viral lytic gene expression. Identification of key cellular targets of the conserved herpesvirus kinases will facilitate the development of broadly effective antiviral strategies.

INTRODUCTION

As major human pathogens, herpesviruses establish life-long persistent infections that result in clinical manifestations ranging from mild cold sores to pneumonitis, birth defects, and cancers. Although the α, β, and γ herpesviruses infect different tissues and cause distinct diseases, they confront many of the same challenges in infecting their hosts, reprogramming cell gene expression, sensing and modifying cell-cycle state, and reactivating the lytic life cycle to produce new virions and spread infection (Arvin et al., 2007). Whereas the α, β, and γ mammalian herpesviruses encode latency and transcriptional regulatory genes that are unique to each subfamily, lytic cycle genes, such as those encoding virion structural components and proteins involved in replication of the viral genomes, are more conserved across the order Herpesviridae. Among the conserved gene products are the orthologous serine/threonine protein kinases (UL13, UL97, BGLF4, and ORF36) encoded by herpes simplex type 1 (HSV1), human cytomegalovirus (HCMV), Epstein-Barr virus (EBV), and Kaposi's sarcoma-associated herpesvirus (KSHV), respectively (Gershburg and Pagano, 2008). These kinases are structurally similar to the cellular kinase cdk2 (Romaker et al., 2006) and are recognized to phosphorylate a number of cyclin-dependent kinase cellular targets, including pRb (Hume et al., 2008), condensin (Lee et al., 2007), stathmin (Chen et al., 2010), lamin A/C (Hamirally et al., 2009; Lee et al., 2008; Meng et al., 2010), elongation factor 1 delta (Kato et al., 2001; Kawaguchi and Kato, 2003; Kawaguchi et al., 2003), MCM4 (Kudoh et al., 2006), and p27/KIP1 (Iwahori et al., 2009), as well as viral targets, including KSHV bZIP (RAP) (Izumiya et al., 2007), EBV EBNA1 and virion proteins (Zhu et al., 2009), and HCMV UL69 (Rechter et al., 2009). Deletion of the protein kinases or inhibition of their activity has been shown to impair virus replication of HCMV and EBV in cultured cells (Gershburg et al., 2007; Prichard et al., 1999; Wolf et al., 2001) and to reduce the titer of HSV1 and murine γ herpesvirus 68 (γ-HV68) in infected mice (Shibaki et al., 2001; Tarakanova et al., 2007). Herpesvirus replication takes place against a background of cell-cycle arrest overlaid with a pseudo S phase environment, whereby virus replication becomes dissociated from cellular DNA replication but selectively utilizes machinery normally activated during S phase (Kudoh et al., 2005; Li and Hayward, 2011). The mimicry of cyclin-dependent kinase activity by the conserved herpesvirus protein kinases contributes to the creation of the pseudo S phase replication environment. This includes breakdown of the nuclear membrane, which is required for egress of virus capsids from the nucleus and is dependent in

infected cells on the viral protein kinase phosphorylation of lamin A/C (Hamirally et al., 2009; Lee et al., 2008; Meng et al., 2010).

Herpesvirus infection and lytic replication trigger the cellular DNA damage response. The induced DNA damage response is blunted during the establishment of latent herpesvirus infection, in EBV by the latency protein EBNA3C (Nikitin et al., 2010), and in HSV1 by the ICP0 protein (Lilley et al., 2010a). This attenuation of the response is necessary for effective establishment of viral latency. Conversely, aspects of the DNA damage pathway are selectively incorporated into the herpesvirus lytic replication program (Gaspar and Shenk, 2006; Kudoh et al., 2005; Lilley et al., 2005; Shin et al., 2006) and are necessary for efficient viral replication. In particular, early events such as activation of the DNA damage response kinase, ataxia telangiectasia mutated (ATM) protein, and phosphorylation of the ATM target H2AX are detected in cells undergoing lytic herpesvirus replication. The γ-HV68 protein kinase (orf36) and the EBV protein kinase BGLF4 have been shown to phosphorylate and activate ATM and H2AX (Tarakanova et al., 2007).

The nucleoside analog drugs acyclovir and ganciclovir, which are used to treat herpesvirus infections, require a monophosphorylation step that occurs in herpesvirus infected cells, but not in uninfected cells, and conserved protein kinases can mediate this phosphorylation (Gershburg et al., 2004; Meng et al., 2010; Moore et al., 2001; Sullivan et al., 1992). The multiple contributions of the conserved protein kinases to herpesvirus replication and spread also make these kinases potential antiviral drug targets, although to date, only one inhibitor of protein kinase enzymatic activity, maribavir, has entered clinical trials (Prichard, 2009).

The herpesvirus protein kinases have a broader substrate recognition than cellular cdks (Baek et al., 2002a; Cano-Monreal et al., 2008; Romaker et al., 2006; Zhu et al., 2009) and neither the full range of their substrates, nor the degree to which the substrates of individual conserved protein kinases overlap, is known. Comprehensive knowledge of common host targets would provide valuable insight into key host factors that facilitate herpesvirus replication and identify signaling pathways whose targeting in combination could enhance the effectiveness of antiviral treatments. Using a human protein microarray screen, we have identified more than 100 shared substrates of the α, β, and γ herpesvirus conserved kinases. Bioinformatic analyses of these shared substrates revealed a statistical enrichment of proteins involved in the DNA damage response. Follow-up experimentation highlighted the key contribution to herpesvirus replication of protein kinase-mediated-phosphorylation of the histone acetlytransferase TIP60, a regulator of the DNA damage response and of chromatin remodeling.

RESULTS

Common Host Substrate Identification for Conserved Herpesvirus Protein Kinases

To identify common substrates for the herpesvirus-conserved protein kinases, we performed assays on a human protein microarray composed of 4,191 unique human proteins, using the UL13, UL97, BGLF4, and ORF36 orthologous kinases encoded by the α, β, and γ viruses HSV1, HCMV, and EBV and KSHV, respectively (Figure 1A). Using normalized amounts of purified viral kinases, as determined by autophosphorylation reactions, we identified 273, 178, 290, and 294 substrates of BGLF4, ORF36, UL97, and UL13, respectively, at a cutoff value of SD $\geq$ 3 (Figure 1A and Figure S1 and Table S1 available online). Of the 643 nonredundant substrates collectively identified by the four kinases, 110 are shared by at least three kinases (Figure 1B). Gene ontology (GO) analysis of these 110 common substrates revealed involvement in eight major functional classes, whereas statistical analysis indicated that the DDR was significantly enriched ($p = 0.004$; hypergeometric test) (Figures 1B and 1C). In addition, proteins in this DDR category are also enriched for known association with viral infections ($p = 0.016$; Table S2).

An effective means for a virus to exploit the host is to target a master regulator that controls multiple downstream signaling pathways. To identify such a master regulator, we applied orthogonal analysis to the shared substrates by incorporating different types of data (e.g., protein-protein and enzyme-substrate interactions) and found a highly connected cluster of 12 proteins, all involved in the DDR (Figure 1C). Intriguingly, several proteins are either the direct targets (e.g., CHK1, RPA1, and RAD51) or downstream effectors of ATM kinase, which plays a crucial role in DDR (Harper and Elledge, 2007). ATM was not present on our protein microarrays. However, recent studies have shown that the activation of ATM's kinase activity in response to DNA damage is dependent upon TIP60 (Sun et al., 2005), one of the substrates that was common to the herpesvirus-conserved protein kinases (Figure 1C). Because TIP60 plays an important role in both DDR and transcription regulation through chromatin remodeling (Sapountzi et al., 2006; Squatrito et al., 2006), it is a candidate master regulator of the herpesvirus life cycle. Therefore, we focused on TIP60 and its role in herpesvirus replication.

EBV BGLF4 Regulates Lytic Replication through the Phosphorylation and Activation of TIP60

Choosing EBV as the primary model, we first tested whether TIP60 expression affected viral DNA replication. Both Akata (EBV^+) B cells and SNU719 (EBV^+) gastric carcinoma cells were transformed with individual shRNA lentiviral constructs to knock down TIP60 expression. As a surrogate for viral DNA replication, we measured the EBV genome copy following lytic induction of EBV by IgG crosslinking and bortezomib treatment, respectively. Knockdown of TIP60 was incomplete (Figure S2) but, nonetheless, reduced the number of EBV genomes by 60%–80% on both cell backgrounds and with both lytic induction treatments (Figure 2A). Measurement of extracellular infectious virus found an ~90% reduction upon TIP60 silencing (Figure 2B). Because the observed decrease was shown with two different shRNAs, the phenotype is unlikely to be due to off-target shRNA effects. These results indicate that TIP60 is a physiologically relevant substrate in the EBV life cycle.

To demonstrate that TIP60 is a target of the EBV kinase BGLF4 in cells, we first showed that TIP60 interacted with both a wild-type (WT) BGLF4 and a kinase-dead mutant ($BGLF4^{KD}$) in transfected cells using reciprocal coimmunoprecipitations (co-IPs) (Figures 3A and S3A). Note that, though the loss of BGLF4 kinase activity did not affect its interaction with TIP60, there was a change in TIP60 mobility with $BGLF4^{KD}$, indicating that BGLF4

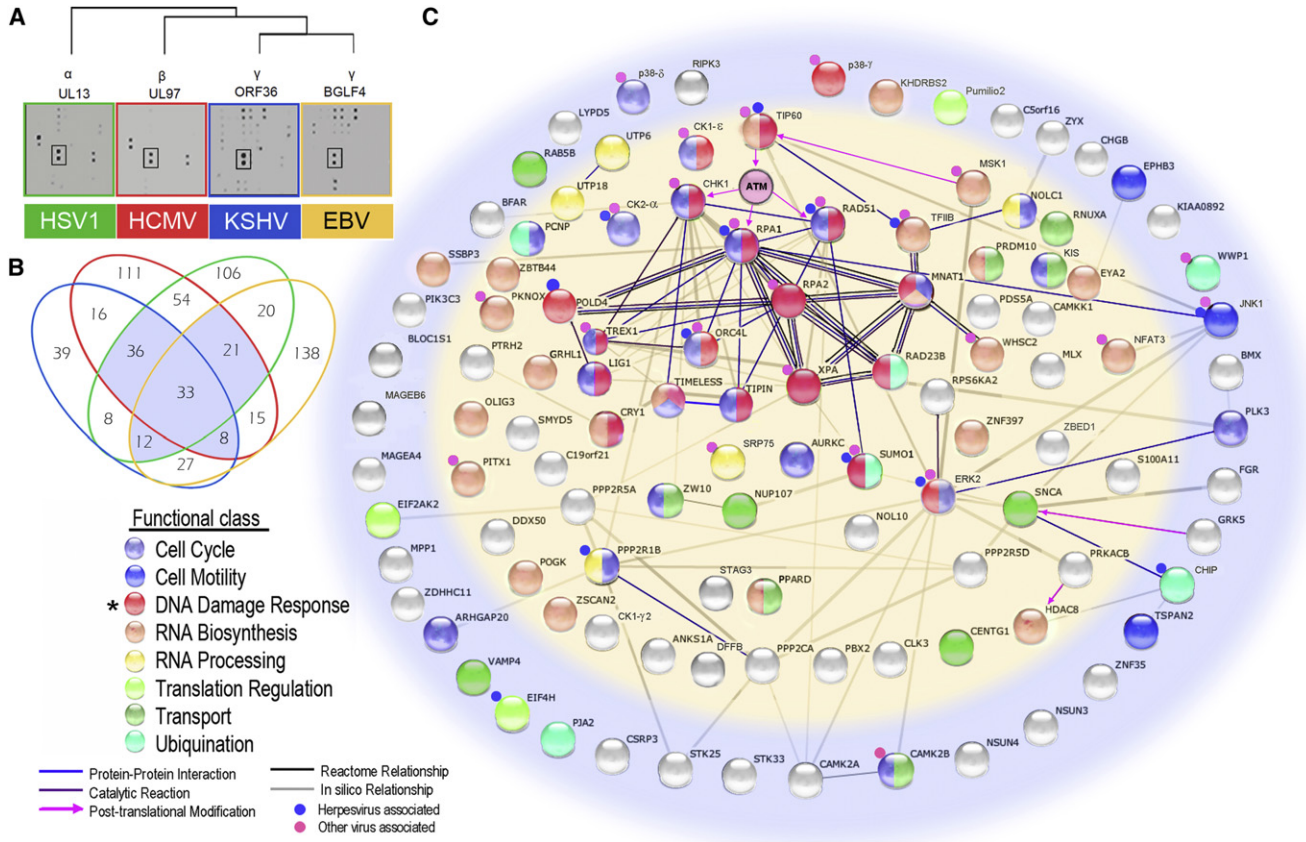

Figure 1. Identification of Common Host Protein Substrates for α, β, and γ Human Herpesvirus Protein Kinases: Enrichment of Proteins in the DNA Damage Pathway

(A) Autoradiograph showing representative sections of typical protein array phosphorylation assays performed using the four viral kinases. All substrates are printed in duplicate. The rectangle highlights a common substrate, Pumilio2.

(B) Venn diagram illustrating the overlap in substrate specificity of the herpesvirus protein kinases. Of 643 total substrates, the highlighted 110 host proteins were phosphorylated by at least three kinases. See also Table S1 and Figure S1.

(C) Interaction network for the 110 shared host proteins. Proteins are color coded by their functional classes. An asterisk indicates the enriched functional class of 19 proteins involved in DDR. Proteins in the inner oval (light yellow) are nuclear proteins. whereas the proteins in the outer ring are in other cellular compartments. Edges between the proteins represent known or predicted connections, such as protein-protein interactions, catalytic reactions, and enzyme-substrate relationships, obtained from the database STRING (http://string-db.org/). Note that ATM was not present on the human protein array. See also Tables S1 and S2.

plays a role in TIP60 phosphorylation. BGLF4-TIP60 interaction during EBV infection was validated using EBV-positive Akata (EBV^+) cells induced into the lytic cycle by treatment with IgG to cross-link the B cell receptor and antibodies against endogenously expressed TIP60 (Figure 3B). Autologous EBV-negative Akata 4E3 cells (EBV^-) served as a negative control. Having shown that BGLF4 directly phosphorylated TIP60 in vitro (Figure S3B), we sought to determine which sites on TIP60 were phosphorylated. In a previous study, phosphorylation at Ser86 and Ser90 of TIP60 was shown to enhance its HAT activity in vitro using histones as substrates. In addition, GSK3β and CDK1/cyclin B were found to in vitro phosphorylate Ser86 and Ser90, respectively (Charvet et al., 2011; Lemercier et al., 2003). Because BGLF4 and CDK1/cyclin B have overlapping substrate recognition (Hume et al., 2008; Zhu et al., 2009), we created TIP60 constructs carrying single or double mutations at Ser86 and Ser90. To show that BGLF4 directly phosphorylates TIP60 at Ser86, an in vitro phosphorylation assay was performed. We found that the TIP60 pSer86-specific antibody detected phosphorylation of WT TIP60, but not phosphorylation of the S86A or S86/90A mutants (Figure 3C). Further, immunoblot analysis of TIP60 coprecipitated from WT TIP60-, S86A-, or S86/90A-transfected cell extracts by anti-BGLF4 antibody revealed that the S86A and S90A mutations each affected TIP60 mobility, with the effects of the double mutation being additive (Figure 3D). Phosphatase treatment increased the mobility of WT TIP60 coprecipitated with WT BGLF4 to equal that of WT TIP60 coprecipitated with $BGLF4^{KD}$ and also equal to that of the S86/90A double mutant. This indicates that TIP60 Ser86/90 are major sites of phosphorylation by BGLF4. To further confirm Ser86 phosphorylation of TIP60 in vivo, we monitored Ser86 phosphorylation of endogenous TIP60 upon induction of WT BGLF4 or $BGLF4^{KD}$ and found that Ser86 phosphorylation was dependent on the presence of BGLF4 kinase activity (Figure 3E, left). These results were further supported in lytically induced Akata (EBV^+) cells, in which Ser86 phosphorylation of TIP60

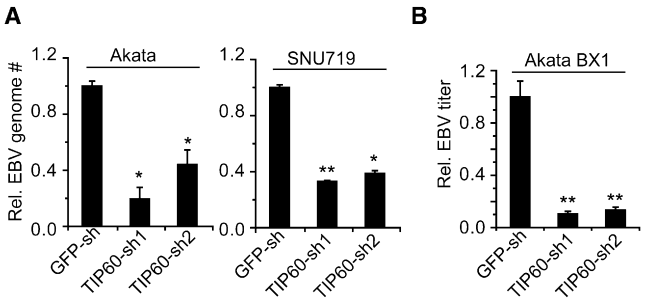

Figure 2. TIP60 Is Required for Efficient EBV Lytic Replication

(A) TIP60 silencing impairs lytic DNA replication. Relative viral genome copy numbers measured by qPCR in lytically induced Akata (EBV$^+$) and SNU719 (EBV$^+$) cells carrying control shRNA (GFP-sh) or TIP60 shRNAs (TIP60-sh1, TIP60-sh2). The experiments were performed in triplicate with ± SD shown. *$p < 0.02$, **$p < 0.01$. See also Figure S2A.

(B) TIP60 silencing reduces infectious virus production. Relative EBV titer produced by lytically induced Akata BX1(EBV$^+$) cells carrying control shRNA (GFP-sh) or TIP60 shRNAs (TIP60-sh1, TIP60-sh2) was measured using Raji cell infection assay. The experiments were carried out in triplicate with ± SD shown. **$p < 0.01$. See also Figure S2B.

was almost completely abolished upon BGLF4 knock down (Figure 3E, right).

To investigate whether the histone acetyltransferase (HAT) activity of TIP60 is affected by BGLF4 phosphorylation, we compared HAT activity of WT and S86/90A TIP60 coexpressed with either WT BGLF4 or BGLF4^{KD}. TIP60 was immunoprecipitated, and its HAT activity was measured in vitro (Figures 3F and S3C). TIP60s HAT activity in the presence of WT BGLF4 was 3-fold greater than that seen with BGLF4^{KD}, indicating that BGLF4's phosphorylation of TIP60 substantially enhances its HAT activity. This result was further supported by the observation that the S86/90A double mutation reduced TIP60's HAT activity to that of a HAT-deficient TIP60 mutant, regardless of the presence or absence of WT BGLF4 or BGLF4^{KD} (Figures 3F and S3C). Taken together, the data establish that BGLF4 interacts with and phosphorylates TIP60 to increase TIP60's HAT activity.

BGLF4 Induces the DNA Damage Response and Chromatin Remodeling through TIP60

TIP60 mediates chromatin remodeling, and TIP60 acetylation of ATM activates ATM autophosphorylation and ATM transphosphorylation of downstream targets such as those illustrated in Figure 4A. Although DDR and chromatin remodeling have been implicated in herpesvirus replication, the molecular mechanisms are poorly understood (Lilley et al., 2010b). Therefore, we examined whether BGLF4 regulates DDR and chromatin remodeling via TIP60. As shown in Figure 4B, the presence of a series of DNA damage markers, including pSer1981 of ATM, pThr68 of CHK2, and pSer139 of histone H2AX (γ-H2AX), is dependent on induction of WT BGLF4, but not BGLF4^{KD}, in Akata (EBV$^+$) cells, and inhibition of ATM abolishes these effects. In addition, Lys5 acetylation of histone H2A (H2AK5^{Ac}), a known target of TIP60, is substantially enhanced upon BGLF4 induction regardless of ATM inhibition (Figure 4B, lanes 5 and 8). Moreover, in a time course of lytic induction in Akata (EBV$^+$) cells, BGLF4 appearance coincides with TIP60 phosphorylation, ATM activation, and γ-H2AX generation (Figure S4A). Consistent with this result, when endogenous BGLF4 is knocked down after lytic induction, ATM Ser1981 autophosphorylation is reduced to the same level as that seen in TIP60 knockdown cells, suggesting that BGLF4-induced DDR depends on TIP60. Moreover, in the same context, the phosphorylation of ATM's downstream effectors, CHK2 (pThr68) and H2AX (pSer139 or γ-H2AX), and the acetylation of TIP60s direct target, H2AK5^{Ac}, are also BGLF4 dependent (Figure 4B, right).

To test whether BGFL4-/TIP60-dependent activation of DDR via ATM plays a role in EBV lytic replication, we measured extracellular virus produced by Akata BX1 (EBV$^+$) cells in the latent state (0 hr) or after lytic induction (48 and 96 hr) in the absence or presence of an ATM inhibitor. We found that EBV lytic replication was suppressed in a dose-dependent manner by ATM inhibition (Figures 4C and S4B), demonstrating the critical role of ATM in EBV lytic replication.

A recent study showed that inhibition of DDR kinases ATM and Chk2 markedly increases the efficiency of EBV latency establishment in B cells (Nikitin et al., 2010). Because TIP60 acts upstream of ATM and CHK2, we asked whether inhibition of TIP60 also increases EBV latency establishment. Using the GFP-tagged virus produced by Akata BX1 cells and a Raji B cell infection assay, we found that latency establishment was increased in Raji cells carrying TIP60 shRNA compared to cells carrying control shRNA (Figures 4D and S4C).

BGLF4 Induces the Expression of Key Lytic Viral Genes through TIP60

To further illustrate the integration of BGLF4 and DDR into EBV DNA replication, we demonstrated that BGLF4 was recruited to the EBV lytic replication origin (OriLyt) upon lytic induction and that its presence induced the recruitment of γ-H2AX and the accumulation of H2AK5^{Ac} at the same locus (Figure 4E). Because TIP60 is known to acetylate histones and regulate gene expression (Avvakumov and Côté, 2007; Baek et al., 2002b; Ikura et al., 2000), we reasoned that the accumulation of H2AK5^{Ac} at this promoter induced by TIP60 could also contribute to viral gene expression. Therefore, we investigated whether the OriLyt (*BHLF1*) promoter or other promoters are targeted by TIP60 during lytic induction.

We performed chromatin immunoprecipitation (ChIP) assays coupled with real-time PCR to quantitatively survey 18-well-annotated EBV promoter regions, including the OriLyt (*BHLF1*) promoter, for TIP60 occupancy. The selected promoters are distributed across the EBV genome (de Jesus et al., 2003) and control 22 EBV genes (Figure 5A). Using antibody against endogenous TIP60 in lytically induced Akata (EBV$^+$) cells, we found that TIP60 associated with the *BHLF1* (*OriLyt*) and *RTA* promoters and also with both promoters (ED-L1 and L1-TR) that regulate *LMP1* (Figure 5A), whereas no significant enrichment of TIP60 was observed on the other tested promoters. These results indicate that TIP60 associates with specific EBV promoters. We next examined the dynamics of this relationship to compare TIP60 occupancy of the *BHLF1* (*OriLyt*), *RTA*, and *LMP1* promoters during latency and postlytic induction. TIP60 association was not detected during latent infection of Akata (EBV$^+$) cells, but TIP60 was recruited to all three promoters at 12 hr postinduction and remained associated at 24 hr (Figure 5B, top). In contrast, the

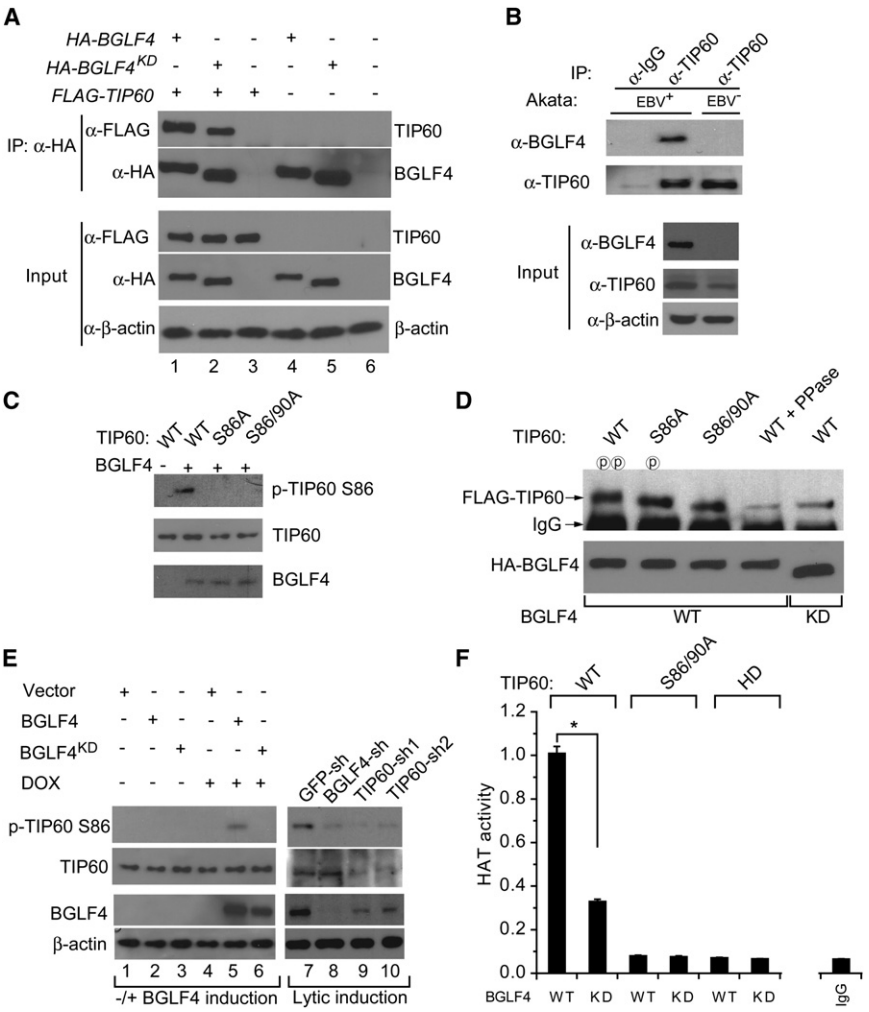

Figure 3. BGLF4 Interacts with, Phosphorylates, and Activates TIP60

(A) Both EBV BGLF4 and kinase-dead BGLF4 interact with TIP60. Western blot analysis of transfected 293T cell extracts showing coprecipitation of TIP60 with BGLF4. BGLF4^{KD}, BGLF4 kinase-dead mutant. Input, 2% whole-cell lysate used for IP. See also Figure S3A.

(B) Interaction between endogenous TIP60 and EBV BGLF4. Lytically induced Akata (EBV$^+$) and Akata 4E3 (EBV$^-$) cell extracts were immunoprecipitated with control IgG or anti-TIP60 antibodies, and the precipitated proteins were immunoblotted with the indicated antibodies. Input, 1% whole-cell lysate used for IP.

(C) BGLF4 phosphorylates TIP60 at S86 in vitro. Western blot analysis after in vitro phosphorylation reactions with indicated combinations of BGLF4 and wild-type or mutant TIP60.

(D) TIP60 Ser86 (S86) and Ser90 (S90) are substrates for BGLF4. Immunoblot comparing the mobility of BGLF4- and kinase-dead BGLF4-coprecipitated wild-type and mutant FLAG-TIP60 with and without phosphatase treatment. 293T cells were transfected as indicated and then treated with 20 μM roscovitine for 12 hr before harvest. See also Figure S3B.

(E) BGLF4 induces TIP60 S86 phosphorylation in vivo. Western blot analysis of cell extracts from Akata (EBV$^+$) cells carrying empty vector, BGLF4, or BGLF4^{KD}, with or without doxycycline (DOX, 20 ng/ml) treatment, and cell extracts from lytically induced Akata (EBV$^+$) cells carrying control GFP, BGLF4, or TIP60 shRNAs.

(F) BGLF4 increases TIP60 HAT activity. Relative HAT activity of wild-type TIP60 (WT), phosphorylation-deficient TIP60 (S86/90A), and HAT-dead TIP60 (HD) immunoprecipitated from 293T cells transfected with wild-type BGLF4 (WT) or BGLF4^{KD} (KD) constructs. The experiments were carried out in triplicate with ± SD shown. *$p < 0.01$. Immunoprecipitated TIP60 loading controls are shown in Figure S3C.

BMRF1 lytic promoter was not occupied by TIP60 during the course of lytic induction. To determine BGLF4's role in this process, we used shRNA lentiviral constructs to knock down BGLF4 expression in Akata (EBV$^+$) B cells and then examined TIP60's recruitment to the *BHLF1*, *RTA*, and *LMP1* promoters during the course of EBV lytic induction (Figure 5B, middle). Quantitative measurement by qPCR showed that TIP60's occupancy on the three promoters was reduced by at least 50% between 12 and 24 hr postinduction (Figure S5A). Thus, BGLF4 enhances TIP60's recruitment to these three viral promoters.

Importantly, the three EBV genes targeted by TIP60 play key roles in viral replication. RTA is one of two key transcriptional activators that drive early and late lytic EBV gene expression (Zalani et al., 1996). The *BHLF1* (*OriLyt*) promoter is an essential component of the viral lytic origin of replication (Schepers et al., 1993). *LMP1* is a latency gene, but its expression is upregulated in the lytic cycle, where LMP1 provides key functions for cell survival and virus release (Ahsan et al., 2005; Dirmeier et al., 2005; Uchida et al., 1999). To correlate TIP60 recruitment and BGLF4 function with the efficiency of expression of these EBV genes, we generated Akata (EBV$^+$) cells that expressed BGLF4 shRNA (BGLF4-sh), TIP60 shRNA (TIP60-sh), or control GFP shRNA (GFP-sh). In the control GFP-sh Akata cells, as expected, these three genes and BMRF1 were highly upregulated at 12 and 24 hr postinduction (Figure 5B, bottom). However, in BGLF4-sh and TIP60-sh cells (Figures 5B, bottom, and S5B), the expression level of *BHLF1*, *RTA*, and *LMP1* was significantly reduced at both time points, whereas *BMRF1* expression was minimally affected. *TIP60* expression was not altered by BGLF4-sh (Figure S5C). Interestingly, *TIP60* knockdown had a greater negative impact than *BGLF4* knock down (Figure 5B, bottom). To summarize, the results reveal that EBV exploits TIP60 via BGLF4 phosphorylation to drive lytic viral gene expression. RTA-induced transcription of BGLF4 leads to reinforced RTA transcription and, consequently, to enhanced expression of the RTA-regulated lytic viral replication program (Wang et al., 2010).

Conserved Role for TIP60 in Herpesvirus Replication

Finally, we tested whether the interplay between the viral kinases and TIP60 is conserved in the other herpesviruses. Using the

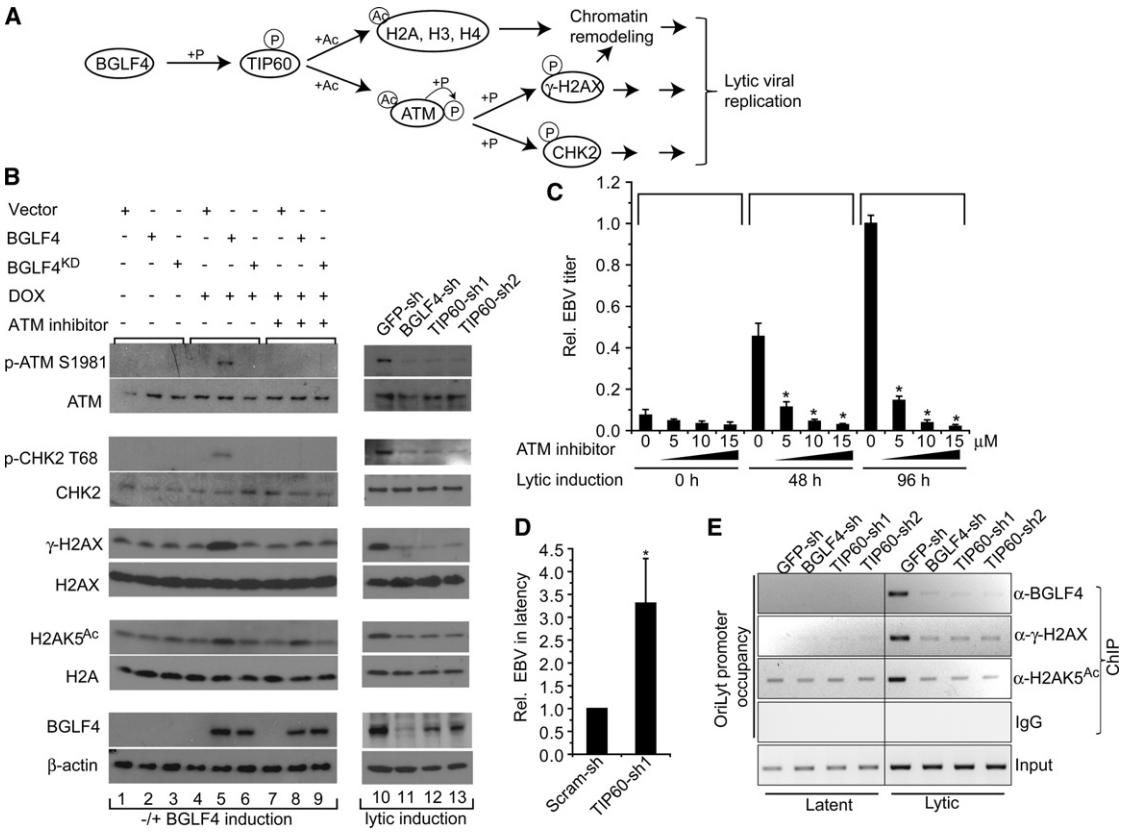

Figure 4. BGLF4 Induces the DNA Damage Response through TIP60

(A) Schematic illustration of BGLF4's potential function in DDR and chromatin remodeling through TIP60 phosphorylation. P, phosphorylation; Ac, acetylation.

(B) BGLF4 induces histone acetylation and ATM activation via TIP60 phosphorylation. Western blot analysis of cell extracts from Akata (EBV$^+$) cells carrying empty vector, BGLF4, or BGLF4^{KD}, with or without doxycycline (DOX, 20 ng/ml) or ATM inhibitor (KU55933, 15 μM) treatment, as indicated, and cell extracts from lytically induced Akata (EBV$^+$) cells carrying control GFP, BGLF4, or TIP60 shRNAs. See also Figure S4A. The data are representative of at least two independent biological replicates.

(C) ATM inhibitor inhibits EBV lytic replication. Relative EBV titer of lytically induced Akata BX1(EBV$^+$) cells in the absence or presence of ATM inhibitor (KU55933), as indicated, was measured using Raji cell infection assay. The experiments were carried out in triplicate with ± SD shown. *$p < 0.01$. See also Figure S4B.

(D) TIP60 knockdown increases the efficiency of EBV latency establishment. EBV BX1 virus was used to infect Raji cells carrying control scramble shRNA (Scram-sh) or TIP60 shRNA (TIP60-sh1). Phorbol-12-myristate-13-acetate (TPA) (20 ng/ml) and sodium butyrate (3 mM) were added 6 days postinfection, and the number of the GFP-positive Raji cells was calculated to determine the efficiency of latency establishment. *$p < 0.01$. See also Figure S4C.

(E) Lytic induction results in the recruitment of BGLF4 and γ-H2AX to the EBV lytic replication origin (OriLyt) promoter and enrichment of histone acetylation (H2A Lys5 acetylation, H2AK5^{Ac}) on this promoter. ChIP-PCR analysis performed on Akata (EBV$^+$) cells carrying indicated shRNAs showing BGLF4, γ-H2AX, and H2AK5^{Ac} enrichment at the OriLyt promoter after lytic induction.

same approaches described above, we showed that KSHV ORF36, HCMV UL97, and, to a lesser extent, HSV1 UL13 phosphorylated and increased the mobility of TIP60 in cotransfected HeLa cells (Figure 6A) and interacted with TIP60 in transfected 293T cells (Figures 6B, 6C, S6A, and S6B). In addition, we tested for recruitment of TIP60 at the HCMV lytic replication origin (OriLyt) and found that, similar to EBV, TIP60 was recruited to HCMV oriLyt at 24, 48, and 96 hr postinfection (hpi) (Figure 6D). Furthermore, knockdown of TIP60 in HCMV-infected cells significantly reduced production of extracellular HCMV virion DNA (Figures 6E and S6C). HCMV lytic replication was also significantly suppressed by an ATM inhibitor in a dose-dependent manner (Figures 6F and S6D), suggesting that the mechanism of inhibition parallels that shown for EBV. These results demonstrate that the viral kinase-TIP60 partnership is conserved and represents a common virus-host interaction.

DISCUSSION

High-throughput technology is emerging as a powerful tool for the discovery of factors involved in pathogen-host interactions (Brass et al., 2009; Calderwood et al., 2007; Karlas et al., 2010; König et al., 2010; Shapira et al., 2009). Here, we took a protein microarray approach to identify enzyme-substrate interactions for four conserved human herpesvirus kinases, with the hypothesis that the common substrates would reveal host pathways that are critical for replication across the herpesvirus family. By analyzing more than 100 shared host substrates, we identified the DDR pathway as a central target of the conserved herpesvirus kinases. Mechanistic studies showed that, in the absence of external DNA damage cues, the EBV kinase phosphorylated and activated the histone acetyltransferase TIP60, an upstream master regulator of DDR. In addition,

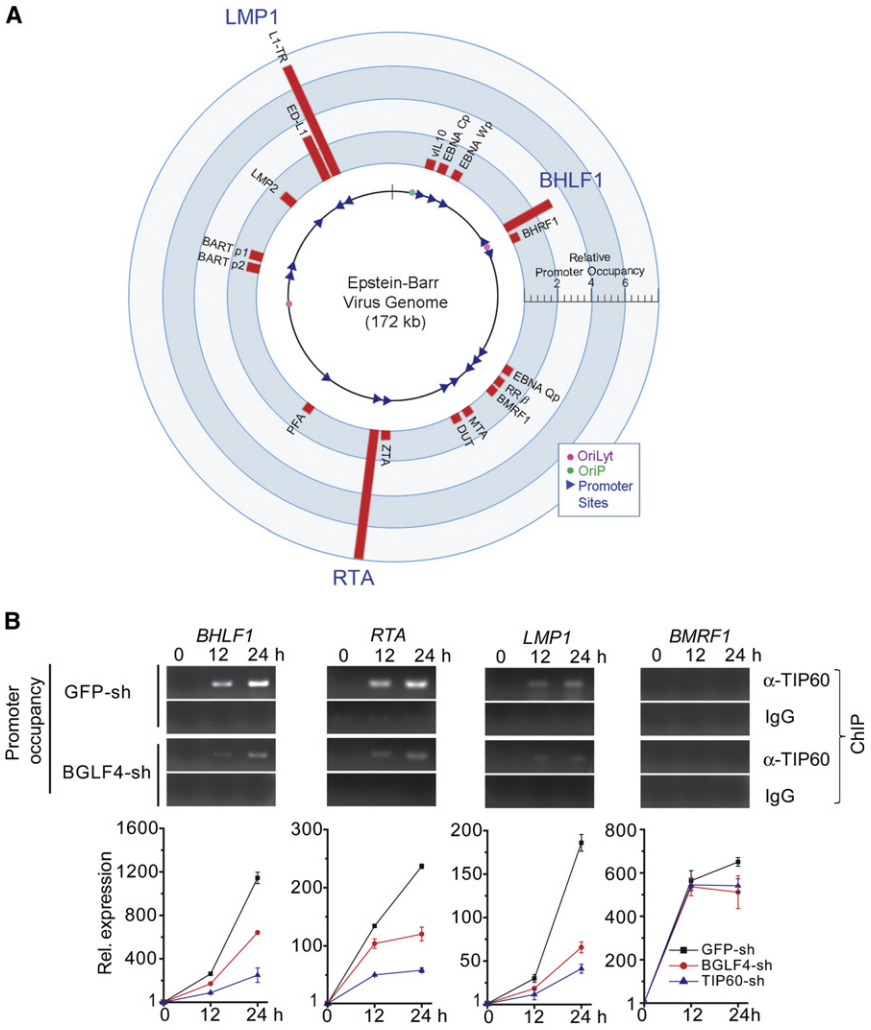

Figure 5. Regulation of EBV Lytic Gene Expression through TIP60

(A) TIP60 recruitment to EBV promoters. The EBV genome annotated with the 18 tested promoters (triangles) and origins of DNA replication (dots). (Red bars) Relative TIP60 occupancy normalized to the IgG control.

(B) Impact of TIP60 recruitment and BGLF4 activity on EBV lytic gene expression. (Top) ChIP-PCR analysis performed on Akata (EBV$^+$) cells showing TIP60 enrichment at the *BHLF1*, *RTA*, and *LMP1* (*L1-TR*) promoters after lytic induction, but not the *BMRF1* lytic promoter. (Middle) Recruitment of TIP60 to the *BHLF1*, *RTA*, and *LMP1* (*L1-TR*) promoters was reduced in BGLF4-sh Akata (EBV$^+$) cells. (Bottom) RT-qPCR analysis of mRNA levels for the corresponding genes and a nonenriched gene (*BMRF1*) in Akata (EBV$^+$) cells carrying the indicated shRNAs. The experiments were carried out in triplicate with ± SD shown. See also Figure S5.

TIP60 was integrated into the virus lytic program by recruitment to the viral chromatin, where TIP60 activated specific EBV genes critical for viral replication.

TIP60 was originally identified as a partner of the HIV type 1 (HIV-1) transactivator, Tat (Kamine et al., 1996), and is targeted by several viruses. Human T cell lymphotropic virus type 1 (HTLV-1) p30^{II} enhances Myc transforming activity through stabilizing Myc-TIP60 transcriptional interactions (Awasthi et al., 2005). TIP60 interaction with viral TAT, E6, and UL27 proteins encoded by HIV-1, human papillomavirus (HPV), and HCMV, respectively, induces TIP60 degradation (Col et al., 2005; Jha et al., 2010; Reitsma et al., 2011), which is believed to enable establishment of viral latency and enhance virus-induced oncogenesis. In the case of HCMV, viruses deleted or mutated for the UL97 protein kinase escape through secondary mutations in the UL27 protein that degrades TIP60 (Chou, 2009; Reitsma et al., 2011). A recent study by Nikitin et al. found that the DDR induced upon EBV infection is a robust host antiviral defense, and EBV employs countermeasures to overcome the growth inhibitory effects of the host DDR in order to establish latency (Nikitin et al., 2010). These authors found that treatment of B cells with an ATM inhibitor increased latency establishment. We find here that TIP60 inhibition with shRNA also increases latency establishment, implying that TIP60 is an upstream mediator of DDR induced upon EBV infection. Interestingly, BGLF4 is present in the EBV tegument (Asai et al., 2006) and, consequently, is introduced into cells upon EBV infection. Therefore, BGLF4 would be available to initiate a transient activation of TIP60, and the DDR and BGLF4/TIP60 partnership may be an important factor in inducing a cellular environment that is hostile to latency establishment.

In counterpoint, we demonstrate that TIP60 plays a positive role in the lytic replication of herpesviruses: TIP60 shRNA significantly reduces virus production from β and γ herpesvirus-infected cells. In the case of EBV, TIP60 HAT activity is enhanced via phosphorylation by the EBV-encoded protein kinase BGLF4 at the same sites that are phosphorylated by CDC2/CDK1 and GSK3β (Charvet et al., 2011; Lemercier et al., 2003). This interaction is sufficient to trigger DDR. DDR plays an important role in the lytic viral life cycle. EBV lytic replication elicits DDR by triggering ATM autophosphorylation and activation. Activated ATM phosphorylates its downstream targets, such as H2AX, p53, CHK2, and RPA2, and phosphorylated ATM, RPA2, and Mre11/Rad50/Nbs1 (MRN) complexes are recruited to replication compartments in nuclei during EBV lytic replication (Kudoh et al., 2005; Kudoh et al., 2009). However, the mechanism of virus-triggered ATM activation has been elusive. Although γ-HV68 kinase orf36 and EBV BGLF4 have been found to directly phosphorylate H2AX, this phosphorylation was reduced significantly in ATM-deficient cells (Tarakanova et al., 2007) and also, as shown here in Figure 4B, in cells treated with an ATM inhibitor. As summarized in Figure 7, our experiments mechanistically link the viral kinases to ATM and its downstream targets CHK2 and H2AX via TIP60.

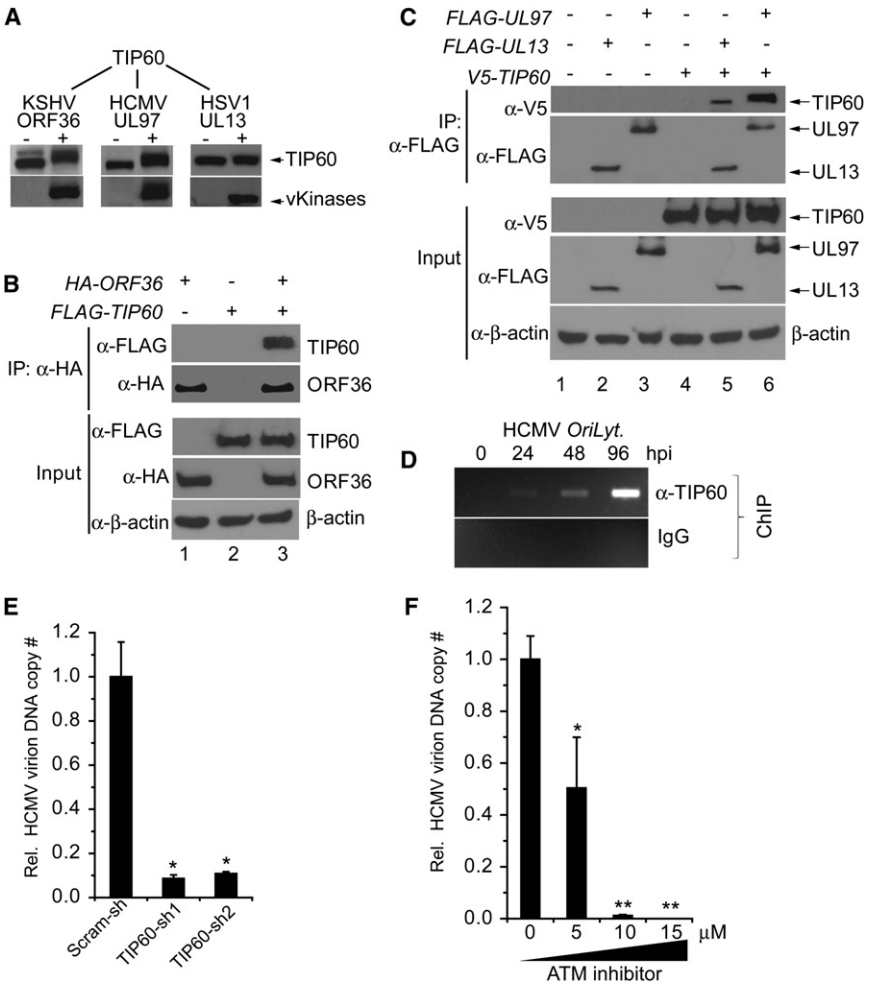

Figure 6. Conserved Role for TIP60 in Herpesvirus Replication

(A) Western blot analysis showing that KSHV ORF36 and HCMV UL97 increase the mobility of TIP60 in transfected HeLa cells.

(B and C) TIP60 coprecipitates with (B) KSHV ORF36, (C) HCMV UL97, and HSV1 UL13 using contransfected 293T cells. Reciprocal immunoprecipitations are presented in Figures S6A and S6B. Input, 2% whole-cell lysate used for IP.

(D) TIP60 is recruited to HCMV lytic replication origin (OriLyt) at 24, 48, and 96 hr postinfection (hpi).

(E) TIP60 is required for efficient HCMV replication. Relative supernatant virion DNA from HCMV-infected HF cells (96 hpi) carrying control scramble shRNA (Scram-sh) or TIP60 shRNA (TIP60-sh) was determined with qPCR. The experiments were carried out in triplicate with ± SD shown. *$p < 0.01$. See also Figure S6C.

(F) ATM inhibitor inhibits HCMV replication. Relative supernatant virion DNA from HCMV-infected HF cells (96 hpi) in the absence or presence of ATM inhibitor (KU55933) was determined with qPCR. The experiments were carried out in triplicate with ± SD shown. *$p < 0.01$, **$p < 0.005$. See also Figure S6D.

We also demonstrate that TIP60 plays a positive role in transcriptional regulation of key lytic viral genes (Figure 7). BGLF4 has been implicated in facilitating viral egress from the nucleus by phosphorylating lamins (Lee et al., 2008). Interestingly, we find that TIP60 is recruited to the *LMP1* promoters after lytic induction and is needed for achieving normal levels of lytic *LMP1* transcription. LMP1 downstream signaling is important for nuclear egress of virions (Ahsan et al., 2005), and our data suggest that TIP60-mediated activation of LMP1 expression represents another mechanism by which BGLF4 promotes this aspect of infectious EBV production. TIP60's negative role in the establishment of latency and its positive role in lytic viral replication place TIP60 at the decision point between viral latency establishment and productive lytic replication (Figures 2 and 4D).

This work illustrates the value of high-throughput, unbiased approaches for the discovery of conserved viral targets. There are few drugs available to treat herpesvirus infections, and viral escape mutants develop upon extensive use of this limited repertoire. The herpesvirus protein kinases are attractive antiviral drug targets. However, developing broadly effectively drugs requires knowledge of their common cellular substrates. The information provided by our common substrate identification will assist in the design of assays for new and broadly effective antiherpesvirus therapeutics.

EXPERIMENTAL PROCEDURES

Kinase Assay

Phosphorylation of proteins on human protein arrays by herpesvirus protein kinases was assayed as previously described (Ptacek et al., 2005; Zhu et al., 2009). The list of the 4,191 unique proteins on this array can be found in Table S2 of Hu et al. (Hu et al., 2009). Detailed information is described in the Supplemental Experimental Procedures.

Immunoprecipitation and ChIP Assays

Cells were transfected using Lipofectamine 2000 (Invitrogen) or calcium phosphate, and the amount of DNA in each sample was equalized using vector DNA. Transfected cells were harvested 48 hr posttransfection, using RIPA lysis buffer (50 mM Tris-HCl [pH 7.4], 150 mM NaCl, 1% (v/v) NP40, 1% (w/v) deoxycholate 0.1% (w/v) SDS, and 1 mM EDTA) containing protease inhibitors and phosphatase cocktail I and II (Sigma) (Li et al., 2007). In Figure 3D, cells were treated with 20 μM roscovitine for 12 hr before harvest to minimize the contribution of CDC2/CDK1. Immunoprecipitation and ChIP were carried out as described previously (Zhu et al., 2009). For phosphatase treatment, the immunoprecipitated complex was resuspended in 1 × NEBuffer and incubated with 10 units of calf intestinal phosphatase (New England Biolabs) at 37°C for 1 hr. The complex was then eluted with Laemmli sample buffer and subsequently analyzed by SDS-PAGE and immunoblotting.

Histone Acetyltransferase Assay

TIP60 HAT activity was assayed using Flag-TIP60, Flag-TIP60S86/90A, and HAT dead Flag-TIP60 immunoprecipitated from 293T cells cotransfected with HA-BGLF4 or HA-BGLF4 kinase-dead mutant. Cells were treated with 20 μM roscovitine for 12 hr before harvest, and TIP60 HAT activity was assayed using the HAT Assay Kit (Millipore) modified according to Sun et al. (2005).

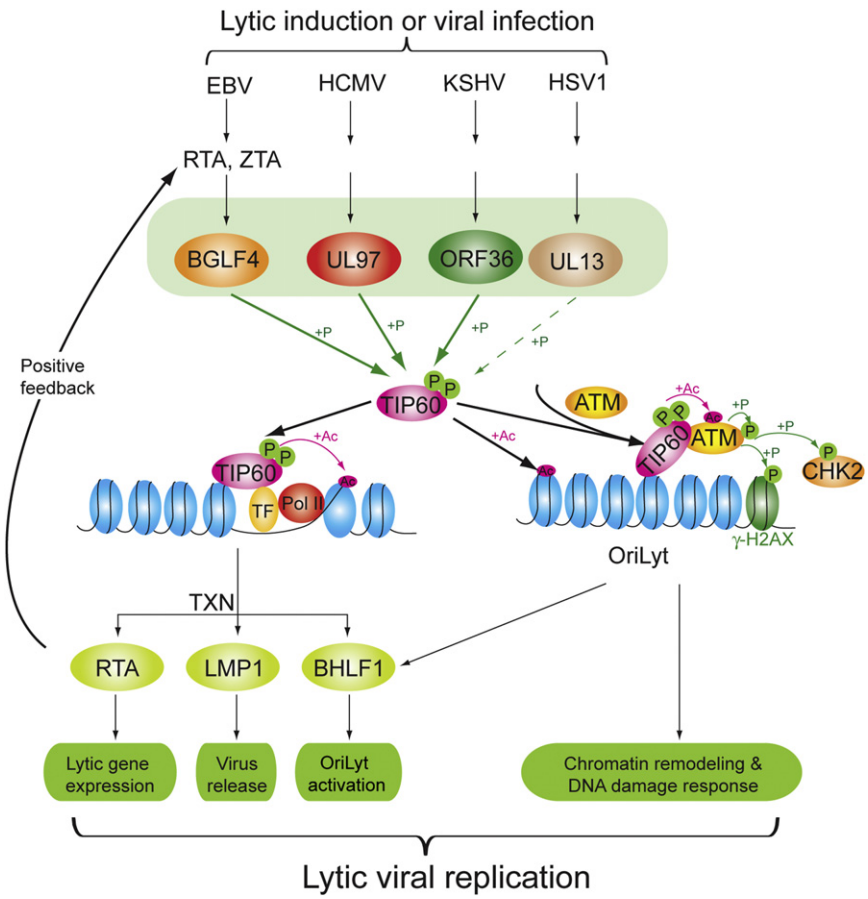

Figure 7. Model for Conserved Herpesvirus Kinases in Regulating Viral Replication through TIP60

The contribution of TIP60 activation by the conserved herpesvirus kinases to lytic replication, as illustrated mechanistically for EBV-infected cells. TXN, transcription; P, phosphorylation; Ac, acetylation; TF, transcription factor; Pol II, RNA polymerase II; OriLyt, lytic replication origin.

Virus Infection

For HCMV infection, HF cells were seeded into 24-well plates 1 day before infection. The cells were washed with PBS, and HCMV-luciferase virus (MOI = 1) was added to each well and incubated for 1.5 hr in 200 μl serum-free Dulbecco's modified Eagle's medium (DMEM). Free viruses were removed with washing, and cells were incubated in medium containing 4% fetal bovine serum for 96 hr. To induce the EBV lytic cycle, Akata (EBV$^+$) cells were treated with 50 μg/ml of goat antihuman IgG (MP Biomedicals) for 24 hr, and SNU719 (EBV$^+$) cells were treated for 24 hr with 20 nM of bortezomib (Fu et al., 2008).

Statistical Analysis

Statistical analyses employed a two-tailed Student's t test. A p value of ≤ 0.05 was considered statistically significant. The data are representative of at least two independent experiments, and values are given as the mean of replicate experiments ± SD.

SUPPLEMENTAL INFORMATION

Supplemental Information includes Supplemental Experimental Procedures, six figures, and two tables and can be found with this article online at doi:10.1016/j.chom.2011.08.013.

ACKNOWLEDGMENTS

J.Z. was supported by American Heart Association Predoctoral Fellowship 0715295U. This work is supported in part by the NIH (R01 CA30356 and R37 CA42245 to S.D.H., R21 CA138163 to S.D.H. and H.Z., RR020839 and R01 GM076102 to H.Z., and R01 EY017589 to J.Q.). We thank Jef Boeke and Seth Blackshaw for critical comments and suggestions and Ravit Arav-Boger and Ran He for assistance with HCMV infection. We also thank Lindsey Hutt-Fletcher for providing recombinant EBV-BX1 virus.

J.Z., R.L., S.D.H., and H.Z. conceived the project. J.Z., R.L., S.D.H., and H.Z. designed experiments. S.D.T., R.F.A., and G.S.H. had input into experimental design. R.L. and J.Z. performed most of the experiments. Z.X., J.L., and J.Q. performed informatics and statistical analyses. S.H. and C.W. generated the human protein arrays. G.L. and M.-R.C. generated reagents. R.L., J.L., J.Z., P.D., and G.S.H. designed and performed HCMV infection assays. H.Z., R.L., J.Z., and S.D.H. wrote the manuscript.

Received: April 5, 2011
Revised: July 25, 2011
Accepted: August 26, 2011
Published: October 19, 2011

REFERENCES

Ahsan, N., Kanda, T., Nagashima, K., and Takada, K. (2005). Epstein-Barr virus transforming protein LMP1 plays a critical role in virus production. J. Virol. *79*, 4415–4424.

Arvin, A., Campadelli-Fiume, G., Mocarski, E., Moore, P.S., Roizman, B., Whitley, R., and Yamanishi, K. (2007). Human Herpesviruses: Biology, Therapy, and Immunoprophylaxis (Cambridge: Cambridge University Press).

Asai, R., Kato, A., Kato, K., Kanamori-Koyama, M., Sugimoto, K., Sairenji, T., Nishiyama, Y., and Kawaguchi, Y. (2006). Epstein-Barr virus protein kinase BGLF4 is a virion tegument protein that dissociates from virions in a phosphorylation-dependent process and phosphorylates the viral immediate-early protein BZLF1. J. Virol. *80*, 5125–5134.

Avvakumov, N., and Côté, J. (2007). The MYST family of histone acetyltransferases and their intimate links to cancer. Oncogene *26*, 5395–5407.

Awasthi, S., Sharma, A., Wong, K., Zhang, J., Matlock, E.F., Rogers, L., Motloch, P., Takemoto, S., Taguchi, H., Cole, M.D., et al. (2005). A human T-cell lymphotropic virus type 1 enhancer of Myc transforming potential stabilizes Myc-TIP60 transcriptional interactions. Mol. Cell. Biol. *25*, 6178–6198.

Baek, M.C., Krosky, P.M., He, Z., and Coen, D.M. (2002a). Specific phosphorylation of exogenous protein and peptide substrates by the human cytomegalovirus UL97 protein kinase. Importance of the P+5 position. J. Biol. Chem. *277*, 29593–29599.

Baek, S.H., Ohgi, K.A., Rose, D.W., Koo, E.H., Glass, C.K., and Rosenfeld, M.G. (2002b). Exchange of N-CoR corepressor and Tip60 coactivator complexes links gene expression by NF-kappaB and beta-amyloid precursor protein. Cell *110*, 55–67.

Brass, A.L., Huang, I.C., Benita, Y., John, S.P., Krishnan, M.N., Feeley, E.M., Ryan, B.J., Weyer, J.L., van der Weyden, L., Fikrig, E., et al. (2009). The IFITM proteins mediate cellular resistance to influenza A H1N1 virus, West Nile virus, and dengue virus. Cell *139*, 1243–1254.

Calderwood, M.A., Venkatesan, K., Xing, L., Chase, M.R., Vazquez, A., Holthaus, A.M., Ewence, A.E., Li, N., Hirozane-Kishikawa, T., Hill, D.E., et al. (2007). Epstein-Barr virus and virus human protein interaction maps. Proc. Natl. Acad. Sci. USA *104*, 7606–7611.

Cano-Monreal, G.L., Tavis, J.E., and Morrison, L.A. (2008). Substrate specificity of the herpes simplex virus type 2 UL13 protein kinase. Virology *374*, 1–10.

Charvet, C., Wissler, M., Brauns-Schubert, P., Wang, S.J., Tang, Y., Sigloch, F.C., Mellert, H., Brandenburg, M., Lindner, S.E., Breit, B., et al. (2011). Phosphorylation of Tip60 by GSK-3 determines the induction of PUMA and apoptosis by p53. Mol. Cell *42*, 584–596.

Chen, P.W., Lin, S.J., Tsai, S.C., Lin, J.H., Chen, M.R., Wang, J.T., Lee, C.P., and Tsai, C.H. (2010). Regulation of microtubule dynamics through phosphorylation on stathmin by Epstein-Barr virus kinase BGLF4. J. Biol. Chem. *285*, 10053–10063.

Chou, S. (2009). Diverse cytomegalovirus UL27 mutations adapt to loss of viral UL97 kinase activity under maribavir. Antimicrob. Agents Chemother. *53*, 81–85.

Col, E., Caron, C., Chable-Bessia, C., Legube, G., Gazzeri, S., Komatsu, Y., Yoshida, M., Benkirane, M., Trouche, D., and Khochbin, S. (2005). HIV-1 Tat targets Tip60 to impair the apoptotic cell response to genotoxic stresses. EMBO J. *24*, 2634–2645.

de Jesus, O., Smith, P.R., Spender, L.C., Elgueta Karstegl, C., Niller, H.H., Huang, D., and Farrell, P.J. (2003). Updated Epstein-Barr virus (EBV) DNA sequence and analysis of a promoter for the BART (CST, BARF0) RNAs of EBV. J. Gen. Virol. *84*, 1443–1450.

Dirmeier, U., Hoffmann, R., Kilger, E., Schultheiss, U., Briseño, C., Gires, O., Kieser, A., Eick, D., Sugden, B., and Hammerschmidt, W. (2005). Latent membrane protein 1 of Epstein-Barr virus coordinately regulates proliferation with control of apoptosis. Oncogene *24*, 1711–1717.

Fu, D.X., Tanhehco, Y., Chen, J., Foss, C.A., Fox, J.J., Chong, J.M., Hobbs, R.F., Fukayama, M., Sgouros, G., Kowalski, J., et al. (2008). Bortezomib-induced enzyme-targeted radiation therapy in herpesvirus-associated tumors. Nat. Med. *14*, 1118–1122.

Gaspar, M., and Shenk, T. (2006). Human cytomegalovirus inhibits a DNA damage response by mislocalizing checkpoint proteins. Proc. Natl. Acad. Sci. USA *103*, 2821–2826.

Gershburg, E., and Pagano, J.S. (2008). Conserved herpesvirus protein kinases. Biochim. Biophys. Acta *1784*, 203–212.

Gershburg, E., Marschall, M., Hong, K., and Pagano, J.S. (2004). Expression and localization of the Epstein-Barr virus-encoded protein kinase. J. Virol. *78*, 12140–12146.

Gershburg, E., Raffa, S., Torrisi, M.R., and Pagano, J.S. (2007). Epstein-Barr virus-encoded protein kinase (BGLF4) is involved in production of infectious virus. J. Virol. *81*, 5407–5412.

Hamirally, S., Kamil, J.P., Ndassa-Colday, Y.M., Lin, A.J., Jahng, W.J., Baek, M.C., Noton, S., Silva, L.A., Simpson-Holley, M., Knipe, D.M., et al. (2009). Viral mimicry of Cdc2/cyclin-dependent kinase 1 mediates disruption of nuclear lamina during human cytomegalovirus nuclear egress. PLoS Pathog. *5*, e1000275.

Harper, J.W., and Elledge, S.J. (2007). The DNA damage response: ten years after. Mol. Cell *28*, 739–745.

Hu, S., Xie, Z., Onishi, A., Yu, X., Jiang, L., Lin, J., Rho, H.S., Woodard, C., Wang, H., Jeong, J.S., et al. (2009). Profiling the human protein-DNA interactome reveals ERK2 as a transcriptional repressor of interferon signaling. Cell *139*, 610–622.

Hume, A.J., Finkel, J.S., Kamil, J.P., Coen, D.M., Culbertson, M.R., and Kalejta, R.F. (2008). Phosphorylation of retinoblastoma protein by viral protein with cyclin-dependent kinase function. Science *320*, 797–799.

Ikura, T., Ogryzko, V.V., Grigoriev, M., Groisman, R., Wang, J., Horikoshi, M., Scully, R., Qin, J., and Nakatani, Y. (2000). Involvement of the TIP60 histone acetylase complex in DNA repair and apoptosis. Cell *102*, 463–473.

Iwahori, S., Murata, T., Kudoh, A., Sato, Y., Nakayama, S., Isomura, H., Kanda, T., and Tsurumi, T. (2009). Phosphorylation of p27Kip1 by Epstein-Barr virus protein kinase induces its degradation through SCFSkp2 ubiquitin ligase actions during viral lytic replication. J. Biol. Chem. *284*, 18923–18931.

Izumiya, Y., Izumiya, C., Van Geelen, A., Wang, D.H., Lam, K.S., Luciw, P.A., and Kung, H.J. (2007). Kaposi's sarcoma-associated herpesvirus-encoded protein kinase and its interaction with K-bZIP. J. Virol. *81*, 1072–1082.

Jha, S., Vande Pol, S., Banerjee, N.S., Dutta, A.B., Chow, L.T., and Dutta, A. (2010). Destabilization of TIP60 by human papillomavirus E6 results in attenuation of TIP60-dependent transcriptional regulation and apoptotic pathway. Mol. Cell *38*, 700–711.

Kamine, J., Elangovan, B., Subramanian, T., Coleman, D., and Chinnadurai, G. (1996). Identification of a cellular protein that specifically interacts with the essential cysteine region of the HIV-1 Tat transactivator. Virology *216*, 357–366.

Karlas, A., Machuy, N., Shin, Y., Pleissner, K.P., Artarini, A., Heuer, D., Becker, D., Khalil, H., Ogilvie, L.A., Hess, S., et al. (2010). Genome-wide RNAi screen identifies human host factors crucial for influenza virus replication. Nature *463*, 818–822.

Kato, K., Kawaguchi, Y., Tanaka, M., Igarashi, M., Yokoyama, A., Matsuda, G., Kanamori, M., Nakajima, K., Nishimura, Y., Shimojima, M., et al. (2001). Epstein-Barr virus-encoded protein kinase BGLF4 mediates hyperphosphorylation of cellular elongation factor 1delta (EF-1delta): EF-1delta is universally modified by conserved protein kinases of herpesviruses in mammalian cells. J. Gen. Virol. *82*, 1457–1463.

Kawaguchi, Y., and Kato, K. (2003). Protein kinases conserved in herpesviruses potentially share a function mimicking the cellular protein kinase cdc2. Rev. Med. Virol. *13*, 331–340.

Kawaguchi, Y., Kato, K., Tanaka, M., Kanamori, M., Nishiyama, Y., and Yamanashi, Y. (2003). Conserved protein kinases encoded by herpesviruses and cellular protein kinase cdc2 target the same phosphorylation site in eukaryotic elongation factor 1delta. J. Virol. *77*, 2359–2368.

König, R., Stertz, S., Zhou, Y., Inoue, A., Hoffmann, H.H., Bhattacharyya, S., Alamares, J.G., Tscherne, D.M., Ortigoza, M.B., Liang, Y., et al. (2010). Human host factors required for influenza virus replication. Nature *463*, 813–817.

Kudoh, A., Fujita, M., Zhang, L., Shirata, N., Daikoku, T., Sugaya, Y., Isomura, H., Nishiyama, Y., and Tsurumi, T. (2005). Epstein-Barr virus lytic replication elicits ATM checkpoint signal transduction while providing an S-phase-like cellular environment. J. Biol. Chem. *280*, 8156–8163.

Kudoh, A., Daikoku, T., Ishimi, Y., Kawaguchi, Y., Shirata, N., Iwahori, S., Isomura, H., and Tsurumi, T. (2006). Phosphorylation of MCM4 at sites inactivating DNA helicase activity of the MCM4-MCM6-MCM7 complex during Epstein-Barr virus productive replication. J. Virol. *80*, 10064–10072.

Kudoh, A., Iwahori, S., Sato, Y., Nakayama, S., Isomura, H., Murata, T., and Tsurumi, T. (2009). Homologous recombinational repair factors are recruited and loaded onto the viral DNA genome in Epstein-Barr virus replication compartments. J. Virol. *83*, 6641–6651.

Lee, C.P., Chen, J.Y., Wang, J.T., Kimura, K., Takemoto, A., Lu, C.C., and Chen, M.R. (2007). Epstein-Barr virus BGLF4 kinase induces premature

chromosome condensation through activation of condensin and topoisomerase II. J. Virol. *81*, 5166–5180.

Lee, C.P., Huang, Y.H., Lin, S.F., Chang, Y., Chang, Y.H., Takada, K., and Chen, M.R. (2008). Epstein-Barr virus BGLF4 kinase induces disassembly of the nuclear lamina to facilitate virion production. J. Virol. *82*, 11913–11926.

Lemercier, C., Legube, G., Caron, C., Louwagie, M., Garin, J., Trouche, D., and Khochbin, S. (2003). Tip60 acetyltransferase activity is controlled by phosphorylation. J. Biol. Chem. *278*, 4713–4718.

Li, R., and Hayward, S.D. (2011). The Ying-Yang of the virus-host interaction: control of the DNA damage response. Future Microbiol. *6*, 379–383.

Li, R.F., Shang, Y., Liu, D., Ren, Z.S., Chang, Z., and Sui, S.F. (2007). Differential ubiquitination of Smad1 mediated by CHIP: implications in the regulation of the bone morphogenetic protein signaling pathway. J. Mol. Biol. *374*, 777–790.

Lilley, C.E., Carson, C.T., Muotri, A.R., Gage, F.H., and Weitzman, M.D. (2005). DNA repair proteins affect the lifecycle of herpes simplex virus 1. Proc. Natl. Acad. Sci. USA *102*, 5844–5849.

Lilley, C.E., Chaurushiya, M.S., Boutell, C., Landry, S., Suh, J., Panier, S., Everett, R.D., Stewart, G.S., Durocher, D., and Weitzman, M.D. (2010a). A viral E3 ligase targets RNF8 and RNF168 to control histone ubiquitination and DNA damage responses. EMBO J. *29*, 943–955.

Lilley, C.E., Chaurushiya, M.S., and Weitzman, M.D. (2010b). Chromatin at the intersection of viral infection and DNA damage. Biochim. Biophys. Acta *1799*, 319–327.

Meng, Q., Hagemeier, S.R., Fingeroth, J.D., Gershburg, E., Pagano, J.S., and Kenney, S.C. (2010). The Epstein-Barr virus (EBV)-encoded protein kinase, EBV-PK, but not the thymidine kinase (EBV-TK), is required for ganciclovir and acyclovir inhibition of lytic viral production. J. Virol. *84*, 4534–4542.

Moore, S.M., Cannon, J.S., Tanhehco, Y.C., Hamzeh, F.M., and Ambinder, R.F. (2001). Induction of Epstein-Barr virus kinases to sensitize tumor cells to nucleoside analogues. Antimicrob. Agents Chemother. *45*, 2082–2091.

Nikitin, P.A., Yan, C.M., Forte, E., Bocedi, A., Tourigny, J.P., White, R.E., Allday, M.J., Patel, A., Dave, S.S., Kim, W., et al. (2010). An ATM/Chk2-mediated DNA damage-responsive signaling pathway suppresses Epstein-Barr virus transformation of primary human B cells. Cell Host Microbe *8*, 510–522.

Prichard, M.N. (2009). Function of human cytomegalovirus UL97 kinase in viral infection and its inhibition by maribavir. Rev. Med. Virol. *19*, 215–229.

Prichard, M.N., Gao, N., Jairath, S., Mulamba, G., Krosky, P., Coen, D.M., Parker, B.O., and Pari, G.S. (1999). A recombinant human cytomegalovirus with a large deletion in UL97 has a severe replication deficiency. J. Virol. *73*, 5663–5670.

Ptacek, J., Devgan, G., Michaud, G., Zhu, H., Zhu, X., Fasolo, J., Guo, H., Jona, G., Breitkreutz, A., Sopko, R., et al. (2005). Global analysis of protein phosphorylation in yeast. Nature *438*, 679–684.

Rechter, S., Scott, G.M., Eickhoff, J., Zielke, K., Auerochs, S., Müller, R., Stamminger, T., Rawlinson, W.D., and Marschall, M. (2009). Cyclin-dependent kinases phosphorylate the cytomegalovirus RNA export protein pUL69 and modulate its nuclear localization and activity. J. Biol. Chem. *284*, 8605–8613.

Reitsma, J.M., Savaryn, J.P., Faust, K., Sato, H., Halligan, B.D., and Terhune, S.S. (2011). Antiviral inhibition targeting the HCMV kinase pUL97 requires pUL27-dependent degradation of Tip60 acetyltransferase and cell-cycle arrest. Cell Host Microbe *9*, 103–114.

Romaker, D., Schregel, V., Maurer, K., Auerochs, S., Marzi, A., Sticht, H., and Marschall, M. (2006). Analysis of the structure-activity relationship of four herpesviral UL97 subfamily protein kinases reveals partial but not full functional conservation. J. Med. Chem. *49*, 7044–7053.

Sapountzi, V., Logan, I.R., and Robson, C.N. (2006). Cellular functions of TIP60. Int. J. Biochem. Cell Biol. *38*, 1496–1509.

Schepers, A., Pich, D., Mankertz, J., and Hammerschmidt, W. (1993). cis-acting elements in the lytic origin of DNA replication of Epstein-Barr virus. J. Virol. *67*, 4237–4245.

Shapira, S.D., Gat-Viks, I., Shum, B.O., Dricot, A., de Grace, M.M., Wu, L., Gupta, P.B., Hao, T., Silver, S.J., Root, D.E., et al. (2009). A physical and regulatory map of host-influenza interactions reveals pathways in H1N1 infection. Cell *139*, 1255–1267.

Shibaki, T., Suzutani, T., Yoshida, I., Ogasawara, M., and Azuma, M. (2001). Participation of type I interferon in the decreased virulence of the UL13 gene-deleted mutant of herpes simplex virus type 1. J. Interferon Cytokine Res. *21*, 279–285.

Shin, Y.C., Nakamura, H., Liang, X., Feng, P., Chang, H., Kowalik, T.F., and Jung, J.U. (2006). Inhibition of the ATM/p53 signal transduction pathway by Kaposi's sarcoma-associated herpesvirus interferon regulatory factor 1. J. Virol. *80*, 2257–2266.

Squatrito, M., Gorrini, C., and Amati, B. (2006). Tip60 in DNA damage response and growth control: many tricks in one HAT. Trends Cell Biol. *16*, 433–442.

Sullivan, V., Talarico, C.L., Stanat, S.C., Davis, M., Coen, D.M., and Biron, K.K. (1992). A protein kinase homologue controls phosphorylation of ganciclovir in human cytomegalovirus-infected cells. Nature *358*, 162–164.

Sun, Y., Jiang, X., Chen, S., Fernandes, N., and Price, B.D. (2005). A role for the Tip60 histone acetyltransferase in the acetylation and activation of ATM. Proc. Natl. Acad. Sci. USA *102*, 13182–13187.

Tarakanova, V.L., Leung-Pineda, V., Hwang, S., Yang, C.W., Matatall, K., Basson, M., Sun, R., Piwnica-Worms, H., Sleckman, B.P., and Virgin, H.W., 4th. (2007). Gamma-herpesvirus kinase actively initiates a DNA damage response by inducing phosphorylation of H2AX to foster viral replication. Cell Host Microbe *1*, 275–286.

Uchida, J., Yasui, T., Takaoka-Shichijo, Y., Muraoka, M., Kulwichit, W., Raab-Traub, N., and Kikutani, H. (1999). Mimicry of CD40 signals by Epstein-Barr virus LMP1 in B lymphocyte responses. Science *286*, 300–303.

Wang, J.T., Chuang, Y.C., Chen, K.L., Lu, C.C., Doong, S.L., Cheng, H.H., Chen, Y.L., Liu, T.Y., Chang, Y., Han, C.H., et al. (2010). Characterization of Epstein-Barr virus BGLF4 kinase expression control at the transcriptional and translational levels. J. Gen. Virol. *91*, 2186–2196.

Wolf, D.G., Courcelle, C.T., Prichard, M.N., and Mocarski, E.S. (2001). Distinct and separate roles for herpesvirus-conserved UL97 kinase in cytomegalovirus DNA synthesis and encapsidation. Proc. Natl. Acad. Sci. USA *98*, 1895–1900.

Zalani, S., Holley-Guthrie, E., and Kenney, S. (1996). Epstein-Barr viral latency is disrupted by the immediate-early BRLF1 protein through a cell-specific mechanism. Proc. Natl. Acad. Sci. USA *93*, 9194–9199.

Zhu, J., Liao, G., Shan, L., Zhang, J., Chen, M.R., Hayward, G.S., Hayward, S.D., Desai, P., and Zhu, H. (2009). Protein array identification of substrates of the Epstein-Barr virus protein kinase BGLF4. J. Virol. *83*, 5219–5231.